Palaeogeography, Palaeoclimatology, Palaeoecology 603 (2022) 111180

Contents lists available at ScienceDirect

Palaeogeography, Palaeoclimatology, Palaeoecology

journal homepage: www.elsevier.com/locate/palaeo

Middle Miocene (Serravallian) wetland development on the northwest edge of Europe based on palynological analysis of the uppermost Brassington Formation of Derbyshire, United Kingdom

Jessica McCoy [a,*], Tabitha Barrass-Barker [a], Emma P. Hocking [a], Jennifer M.K. O'Keefe [b], James B. Riding [c], Matthew J. Pound [a]

[a] Department of Geography and Environmental Sciences, Northumbria University, Newcastle upon Tyne NE1 8ST, UK
[b] Department of Physics, Earth Science, and Space Systems Engineering, Morehead State University, Morehead, KY 40351, USA
[c] British Geological Survey, Keyworth, Nottingham NG12 5GG, UK

ARTICLE INFO

Editor: Howard Falcon-Lang

Keywords:
Lignite
Climate change
Miocene
Palynology
Vegetation
United Kingdom

ABSTRACT

In this paper, we describe palynological assemblages in the Middle Miocene (Serravallian) Kenslow Member of the Brassington Formation at Bees Nest Pit, near Brassington, Derbyshire, U.K., and infer vegetation types and their palaeoclimate implications. The limited lateral extent of the 1.33 m-thick succession of clay and lignite, and its position surrounding fragments of a large tree trunk, suggests that the succession may have accumulated within a tree throw hole or possibly within a shallow stagnant pond, although aquatic lacustrine palynomorphs have not been identified to confirm this latter hypothesis. The stratigraphical distribution of palynological assemblages, based on 58 samples allows reconstruction of a wetland succession. Two pollen zones were identified using CONISS cluster analysis, and a predominantly warm-temperate and mixed mesophytic forest biome was recognised with *Tsuga* conifer pollen-types being dominant (<42%) in both pollen zones. Changes in the make-up of this forested wetland were in response to local environmental changes rather than major climatic shifts. Wetland development culminated in the formation of a relatively open shrub and reed-dominated mire which produced the lignite-precursor peat. Applying the Co-existence Approach, Mean Annual Temperature was 15.6–21.7 °C and Mean Annual Precipitation was 703–1682 mm indicating a warm-temperate to subtropical palaeoclimate, and both parameters show no significant change through the section. Findings suggest that, following the Middle Miocene Climatic Optimum, the Serravallian climate of the northwestern margin of Europe remained much wetter than Central Europe, where more arid climates have been reconstructed, and this difference may have been due to the influence of the proto-North Atlantic Current.

1. Introduction

The climate of the Miocene (23.03–5.33 Ma) was warmer and wetter than present-day and has been identified as an interval of interest in the IPCC AR6 report (Pound et al., 2012a; Steinthorsdottir et al., 2021; IPCC, 2022). Present-day and modelled carbon dioxide (CO_2) concentrations for the end of the 21st century are comparable to those reconstructed for the Middle Miocene (400–600 ppm), pCO_2 reconstructions being based on stomatal densities and index indicators (Royer, 2001; Beerling et al., 2009; Kürschner et al., 2008; Steinthorsdottir et al., 2019, 2020, 2021). The presence of a reduced Antarctic ice mass, less Northern Hemisphere ice, a near-modern palaeogeography and biota also make the Miocene a significant interval for exploring warmer than present climates and the biota that inhabited them (Pound et al., 2011). Global climates cooled during the Middle Miocene Climate Transition (MMCT: 14.5–12.5 Ma) in a step-like manner with East Antarctic Ice Sheet expansion and corresponding deep ocean cooling of 3 °C, based on benthic foraminiferal $\delta^{18}O$ proxies, but surface air temperatures remained warmer than present day (Flower and Kennett, 1994; Billups and Schrag, 2002; Holbourn et al., 2007; Quaijtaal et al., 2014; Super et al., 2018; Steinthorsdottir et al., 2021). Following the Middle Miocene, sea surface temperature gradients between 42°N and 57°N in the North Atlantic collapsed and remained so until around 7.6 Ma; these flat sea surface temperature gradients were interpreted to be a precursor

* Corresponding author at: Department of Geography and Environmental Sciences, Northumbria University, Newcastle upon Tyne NE1 8ST, UK.
E-mail address: jessica.mccoy@northumbria.ac.uk (J. McCoy).

https://doi.org/10.1016/j.palaeo.2022.111180
Received 27 May 2022; Received in revised form 31 July 2022; Accepted 1 August 2022
Available online 5 August 2022

to the modern North Atlantic Current and kept the mid-latitude North Atlantic relatively warm during the MMCT (Super et al., 2020). Palaeobotanical evidence from the North Atlantic region also points to formation of the North Atlantic Current during the Middle Miocene (Denk et al., 2013; Pound and Riding, 2016; Pound and McCoy, 2021). Across northwest and Central Europe, this interval was characterised by relatively stable mean annual precipitation with extensive wetland environments (van Dam, 2006; Utescher et al., 2021).

The British Isles archipelago formed a northwest-trending peninsula on the European continent during the MMCT (Harzhauser and Piller, 2007; Steinthorsdottir et al., 2021; Gibson et al., 2022). Unfortunately, onshore terrestrial Miocene sediments are not common in this region (Pound et al., 2012a, 2012b; Gibson et al., 2022). Of the three known fossiliferous sites, the St. Agnes Outlier in Cornwall has considerable dating uncertainty (Walsh et al., 1987) and Trwyn y Parc in Anglesey is Langhian, probably pre-MMCT (Pound and McCoy, 2021; Gibson et al., 2022). This only leaves the diachronous Kenslow Member of the Brassington Formation (Serravallian–Tortonian) as a possible comparable environment to those observed in northwest and central Europe (Ivanov et al., 2007a, 2007b; Jiménez-Moreno et al., 2008; Hui et al., 2011; Larsson et al., 2011; Szulc and Worobiec, 2012; Pound et al., 2012b; Velitzelos et al., 2014; Pound and Riding, 2016; Utescher et al., 2017). Previous research on the Kenslow Member at the Kenslow Top Pit has shown a relatively stable palynoflora dated as early Tortonian (Boulter, 1971a-b), although only productive grab samples have been analysed from the Serravallian and late Tortonian Kenslow Member outcrops at the Kenslow Top Pit and Bees' Nest Pit, see Fig. 1 for locations (Pound et al., 2012b; Pound and Riding, 2016).

This study is the first to report a continuous palynological record from the Serravallian portion of the Kenslow Member and provides a unique insight into the terrestrial environments present on an Atlantic peninsula prior to full formation and stabilisation of the North Atlantic Current (Super et al., 2020). In this paper we present the first sequence of 58 palynological samples taken through the lignite and clay unit from the Serravallian Kenslow Member at Bees Nest Pit. These are used to reconstruct the palaeoenvironment and palaeoclimate during the later Serravallian.

2. Geological setting

The Kenslow Member is the uppermost of three members that form the Brassington Formation of Derbyshire and Staffordshire in central England (Figs. 1-2). Preserved in around 60 karstic hollows, the Brassington Formation is dominated by the unfossiliferous Kirkham and Bees Nest members, whilst the fossiliferous Kenslow Member has only been identified at seven locations (Boulter et al., 1971; Boulter, 1971b; Walsh et al., 2018). The Kirkham Member comprises up to 70 m of palaeontologically-barren cream/white and red/brown sands intercalated with pebble layers, and which represent the erosional products from the Triassic sandstone escarpment to the south of Brassington according to Yorke (1954), Boulter et al. (1971), and Walsh et al. (1980, 2018). The Bees Nest Member is around 6 m of varicoloured unfossiliferous clays and silts (Boulter et al., 1971; Ford and Jones, 2007; Walsh et al., 2018). The uppermost Kenslow Member contains plant-bearing grey clays and lignite (Boulter et al., 1971; Walsh et al., 1972; Walsh et al., 1980; O'Keefe et al., 2020). The Kenslow Member is diachronous on pollen evidence (Pound and Riding, 2016). At Bees Nest Pit, near Brassington village, Derbyshire, UK (Fig. 1) this unit is Serravallian, whereas at the Kenslow Top Pit, near Friden, it is of Tortonian in age (Pound et al., 2012b; Pound and Riding, 2016). Both these disused quarries have previously yielded a wide range of palaeobotanical remains, including Cupressaceae seeds, fungal remains, leaves, pollen grains, spores and wood (Boulter and Chaloner, 1970; Boulter, 1970; Boulter et al., 1971; Boulter, 1974; Pound et al., 2012b; Pound and Riding, 2016; Pound et al., 2019; O'Keefe et al., 2020; Table 1).

The Brassington Formation is thought to have formed in an alluvial-fluvial-lacustrine depositional setting before being incorporated into its present-day karstic setting (Boulter et al., 1971; Walsh et al., 1972,

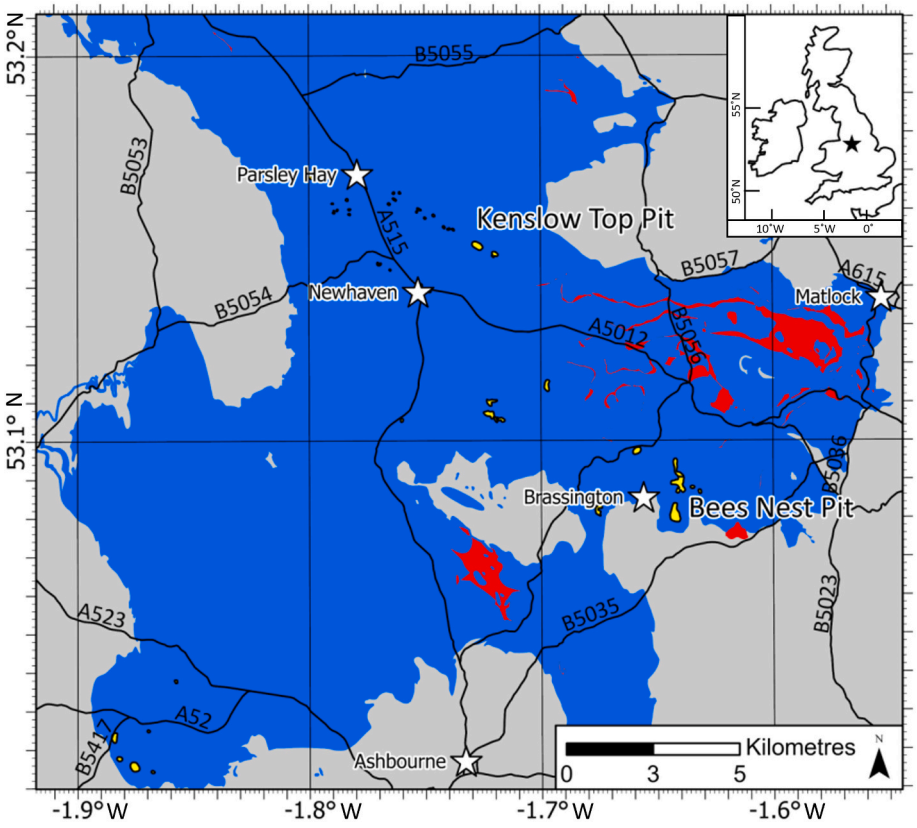

Fig. 1. A simplified geological map of the area where the ~60 known outcrops of the Brassington Formation are located, with an inset map at the top right to illustrate the location of this area in the British Isles. The Brassington Formation is shown in yellow, although most karstic hollows are too small to be visible at this scale and some are visible only as irregular black dots. The Peak Limestone Group (Mississippian/Lower Carboniferous) is shown in blue ornament; the 'pockets' of Brassington Formation are in karstic cavities within this major carbonate unit. The red ornament indicates igneous rocks, dominantly basalt, within the Peak Limestone Group. The grey colour represents several major Pennsylvanian/Upper Carboniferous and Triassic siliciclastic lithostratigraphical units which overlie the Peak Limestone Group in this part of the East Midlands of England. Major roads in the area are included for orientation, together with selected settlements (white stars). The map was generated using ArcGIS Pro. This simplified geological map is based upon the British Geological Survey 1:10000 scale digital geological map (Smith, 2013), using the EDINA Geology Digimap Service. The road network is from the Ordnance Survey Open Roads (SHAPE geospatial data), scale 1:25000, updated on 23 September 2021. Downloaded on 2022-04-13 09:54:41.238. [1.5-column fitting image]. (For interpretation of the references to colour in this figure legend, the reader is referred to the web version of this article.)

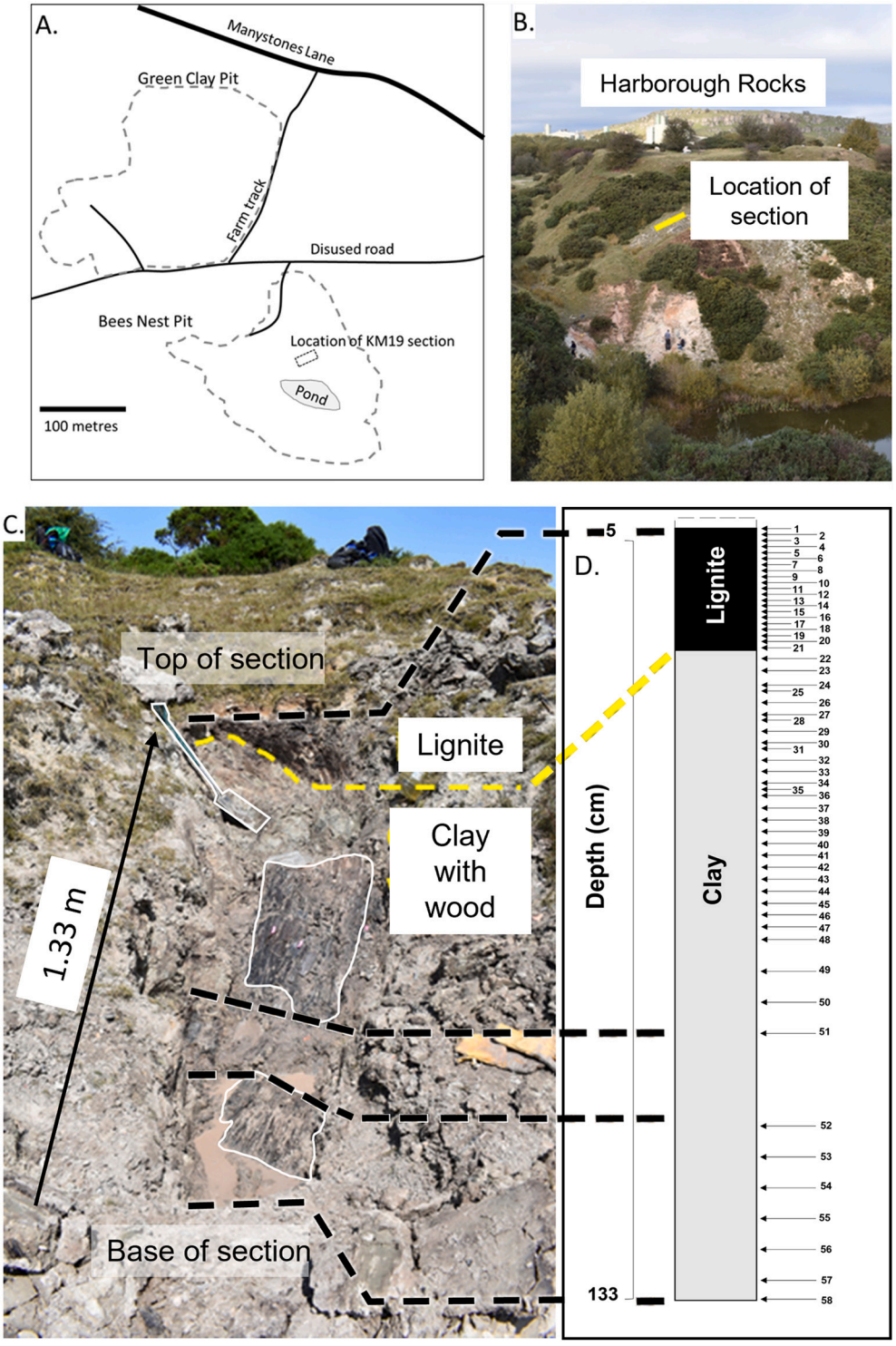

Fig. 2. Location of the KM19 section within the Kenslow Member of the Brassington Formation at Bees Nest Pit. A. Field map of the site showing the location of Bees Nest Pit in relation to Manystones Lane, the nearest access road, and the location of the KM19 section to the north of the pond. B. Field photograph of Bees Nest Pit with the location of the KM19 section highlighted and the location of Harborough Rocks on the north side of Manystones Lane indicated. C. Photograph of the KM19 section with annotated lithology and large fragment of fossil wood in centre of the section (note the spade for scale). D. Lithological log of the KM19 section with palynology samples indicated by arrows; the sample numbers indicate the depth in centimetres. [2-column fitting image].

1980, 2018). Bees Nest Pit and Kenslow Top Pit exhibit structures interpreted to be subsidence-related sag synclines and recent developments in the understanding of hypogene processes suggest post-Miocene uplift triggered suffusion processes (Walsh et al., 1972, 1980, 2018). The setting of the organic-rich Kenslow Member has been proposed to be an isolated lake (Walsh et al., 2018) or a sinkhole pond (Pound et al., 2012b).

2.1. Previous palynological investigations of the Kenslow biostratigraphy

Previous studies have identified a diverse assemblage of >60 pollen and spore taxa from the Kenslow Member at Bees Nest and Kenslow Top pits (Boulter and Chaloner, 1970; Boulter, 1971a-b; Pound et al., 2012b; Pound and Riding, 2016). Boulter (1971a) presented a succession of samples from Kenslow Top Pit that showed a relatively stable pollen and spore assemblage dominated by Ericaceae (<37%), triporates (<30%) and *Tricolpopollenites liblarensis* (<17%). A single sample was also presented from Bees Nest Pit that was dominated by relative abundances of

Table 1
List of pollen microfossils found in previous studies on the Brassington Formation. Names highlighted in bold represent recovered fossilised leaves, * represent recovered seeds. Table is based on findings by Boulter and Chaloner, 1970; Boulter, 1970; Boulter et al., 1971; Boulter, 1974; Pound et al., 2012b; Pound and Riding, 2016; Pound et al., 2019; O'Keefe et al., 2020. Nearest living relatives were assigned using botanical affinities listed by Stuchlik et al. (2001, 2002, 2009, 2014).

Order	Family	Taxa	NLR	Order	Family	Taxa	NLR
Fungi	Chaetosphaeriaceae	*Chaetosphaeria elsikii*	*Chaetosphaeria*			*Tricolpopollenites edmundi*	Anacardiaceae
	Incertae sedis	*Rhexoampullifera stogieana*	*Rhexoampullifera*		Brassicaceae?*	*Parrya* sp.	*Parrya*
		R. sufflata			Compositae	Compositae	Compositae
Bryophyta	Hypnodendraceae	*Hypnodendron* sp.	*Hypnodendron*			*Compositoipollenites rizophorus*	*Compositae*
		Muscites lanceolata	Unknown		Betulaceae	*Alnus* sp.	*Alnus*
	Sphagnaceae	*Stereisporites crucis*	*Sphagnum*			*Carpinus* sp.	*Carpinus*
		S. germanicus rheanus				*Corylus* sp.	*Corylus*
		S. granisteroides				*Trivestibulopollenites betuloides*	*Betula*
		S. magnoides			Caryophyllaceae	Caryophyllaceae	Caryophyllaceae
		S. microzonales			Cyrillaceae	cf. *Cyrilla thompsoni*	*Cyrillaceae/ Clethraceae*
		S. minimoides			Ericaceae	*Calluna* sp.	*Calluna*
		S. minor microstereis				*Empetrum* sp.	*Empetrum*
		S. pliocenious pliocenious				*Erica* sp.	Ericaceae
		S. semigranulus				Ericaceae	
		S. stereoides stereoides				*Ericipites baculatus*	
		S. wehningensis				*E. callidus*	
		S. sp.				*E. costatus*	
Pteridophyta	Lycopodiaceae	*Lycopodium* sp.	*Lycopodium*			*E. ericius*	
	Gleicheniaceae	*Gleicheniidites senonicus*	*Gleichenia*			*Rhododendron* sp.	*Rhododendron*
	Osmundaceae	*Osmunda* sp.	*Osmunda*		Fabaceae?	*Tricolpopollenites ipilensis*	Unknown
	Polypodiaceae	*Laevigatosporites haardtii*	*Polypodium*			*T. libalrensis fallax*	Fabaceae
		Verrucatosporites favus				*T. liblarensis liblarensis*	
	Polypodiaceae (?)	*Leiotriletes wolffi brevis*	*Lygodium*		Fagaceae?	*Quercoidites microhenrici*	Quercus
		Triplanosporites microsinuosus	*Filicopsida*			*Tricolpopollenites microhenrici*	
	Schizaeaceae (?)	*Leiotriletes wolffi wolffi*	*Lygodium*		Hamamelidaceae	*Corylopsis* sp.	*Corylopsis*
	Incertae sedis	*Triplanosporites sinuosus*	*Filicopsida*			*Liquidambar* sp.	*Liquidambar*
Gymnospermae	Cupressaceae	*Cryptomeria anglica*	*Cryptomeria*		*Incertae sedis*	*Tricolpopollenites* sp.	Unknown
		C.* sp.	*japonica*		Juglandaceae	*Carya* sp.	*Carya*
		Cupressaceae	Cupressaceae			*Juglans* sp.	*Juglans*
		Inaperturopollenites hiatus			Liliaceae	*Smilax* sp.	*Smilax*
		I. dubius			Myricaceae	*Myrica* sp.	*Myrica*
	Pinaceae	***Abies alba****	*Abies*		Nyssaceae	*Nyssa* sp.	*Nyssa*
		Abies sp.			Onagraceae	*Corsinipollenites maii*	Onagraceae
		Cathaya sp.	*Cathaya*		Pentaphylacaceae	*Eurya* sp.	*Eurya*
		Cedrus sp.	*Cedrus*		Plumbaginaceae	*Armeria* sp.	Plumbaginaceae
		Keteleeria sp.	*Keteleeria*			*Limonium* sp.	*Limonium*
		Picea sp.*	*Picea*		Poaceae	*Graminidites media*	Poaceae
		Pinus sylvestris* - *type*	*Pinus*		Polemoniaceae	*Polemonium*sp.	*Polemonium*
		P. haploxylon - type			Polygonaceae	*Polygonum* sp.	*Polygonum*
		P. sp.			Rhamnaceae	cf. *Rhamnus* sp.	*Rhamnus*
		***Tsuga canadensis* - type**	*Tsuga*		Rubiaceae	cf. *Rubiaceae*	Rubiaceae
		***T. diversifolia* - type**			Salicaceae	*Salix* sp.	*Salix*
		T. sp.				*Tricolpopollenites retiformis*	
	Podocarpaceae	*Podocapoidites libellus*	*Podocarpus*		Sapindaceae	*Aesculus* sp.	*Aesculus*
		Podocapus-type			Sapotaceae	*Tetracolporopollenites sapotoides*	Sapotaceae
	Sciadopityaceae	*Sciadopitys* sp.	*Sciadopitys*		Saxifragaceae	*Saxifraga* sp.	*Saxifraga*
		Sciadopitys tertiaria			Smilacaceae	*Periporopollenites echinatus*	*Liquidambar*
Angiospermae	Actinidiaceae	*Actinidia* sp.	*Actinidia*		Symplocaceae	*Symplocoipollenites rotundus*	*Symplocos*
	Aquifoliaceae	*Ilex* sp.	*Ilex*			*S. vestibulum*	
		Tricolporopollenites iliacus			Trapaceae	cf. *Trapa* sp.	*Trapa*
		T. margaritas	Aquifoliaceae		Ulmaceae	*Ulmus* sp.	*Ulmus*
	Araliaceae	*Hedera* sp.	*Hedera*			Indeterminate	Unknown

Pinus haploxylon-type (<20%), *Quercoidites microhenrici* (10%) and *Sciadopitys* (8%). Pound et al. (2012b) located an unstudied section of the Kenslow Member at Kenslow Top Pit, which contained a single productive sample that differed from the previous assemblage found by Boulter (1971a). This was dominated by *Compositoipollenites rhizophorus* (20%), *Stereisporites* (12%), *Pinus* (10%), Ericaceae (8%) and *Trivestibulopollenites betuloides* (4%) and led Pound et al. (2012b) to assign a late Tortonian (younger than 9 Ma) date to the entire Kenslow Member. The rediscovery of a Kenslow Member section at Bees Nest Pit (Fig. 1) and fossil wood stored in the British Geological Survey archives, led Pound and Riding (2016) to propose diachronous dates for different Kenslow Member outcrops. The original Kenslow Top Pit of the Kenslow Member outcrop is no longer visible in the field, but wood recovered by Yorke (1961) contained Kenslow Member clay filled cracks. This yielded an assemblage comparable to Boulter (1971a) dominated by Ericaceae pollen types and, notably, *Triplanosporites sinuosus* (Pound and Riding, 2016). The Kenslow Member sample from Bees Nest Pit was found to be dominated by conifer pollen, especially *Cathaya*, *Pinus*, *Sciadopitys* and *Tsuga* (Pound and Riding, 2016). Angiosperms were present, but only *Carya,* Ericaceae and *Ilex* formed significant proportions of the assemblage (Pound and Riding, 2016). Combined with the sample presented in Pound et al. (2012b), it was determined that the palynoflora from the

Kenslow Member at Bees Nest Pit is comparable to the younger Serravallian of the Lower Rhine Basin, whilst the two samples from Kenslow Top Pit are more comparable to the Dutch and German Tortonian (Pound and Riding, 2016). Climatically, this sequence of samples from the different outcrops of the Kenslow Member showed decreasing temperatures, precipitation and seasonality from the late Serravallian to the late Tortonian (Pound et al., 2012b; Pound and Riding, 2016; Gibson et al., 2022). The Kenslow Member at Bees Nest Pit has only ever been studied from grab samples. This presents a major omission in our knowledge of the palaeoenvironments and palaeoclimates of northwest Europe during an interval of abnormal North Atlantic temperature gradients (Super et al., 2020). In this paper we present the first sequence of 58 palynological samples taken through the lignite and clay from the Serravallian Kenslow Member at Bees Nest Pit. These are used to reconstruct the palaeoenvironment and palaeoclimate during the later Serravallian.

3. Materials and methods

A clay and lignite succession, measuring 133 cm-thick, was extracted from the type section of the Kenslow Member at Bees Nest Pit at 53°05′16.9"N, 1°38′28.6"W (Fig. 2). Fifty-eight samples, weighing 1–2 g were taken from 1 to 5 cm intervals along the lignite and clay unit using a sterilised spatula. 17 samples were taken at at 1 cm-intervals from the lignite section (5–21 cm), and 41 samples were taken at 1–5 cm-intervals throughout the clay section (22–133 cm). Succession depths between 90 and 105 cmwere not recovered, hence samples could not be taken for depths 95 and 100 cm.

Twenty-five samples were taken for grain size analysis using the Mastersizer 2000 at 3–5 cm intervals throughout the lignite and clay unit. *Lycopodium* tablets were not added to samples. A non-acid technique was used on samples taken from both the lignite and clay sections, following Riding and Kyffin-Hughes (2006), that involved disaggregating samples in hot water and sieving through 125 μm and 10 μm nylon mesh sieves (Pound et al., 2021; Riding, 2021). Sieved residues were centrifuged at 3300 rpm for 3 min to remove excess water in the supernatant. 1 ml of copper sulphate was added to each sample to prevent microbial growth (Pound et al., 2021).

Pollen samples were then permanently mounted to slides using 0.1 ml of Kaiser's glycerol jelly and a Bunsen burner. Where high silica content obscured the view of palynomorphs (22–133 cm), samples underwent density separation using a watch glass using distilled water to fractionate the silica content from palynomorphs (Pound et al., 2021; Riding, 2021). Floating pollen and spores were pipetted from the upper fraction to be later mounted on permanent slides. Pollen and spores were identified and counted using a Leica DM500 light microscope at x400 magnification. The pollen and spore descriptions of Boulter (1971a) and Stuchlik et al. (2001, 2002, 2009, 2014) were used for taxonomical identifications.

3.1. Palaeoclimate techniques

Nearest living relatives of fossil taxa were determined by botanical affinities listed Stuchlik et al. (2001, 2002, 2009, 2014). Photomicrographs were obtained using an integral ICC50W digital camera operated by Leica Application Suite® (V4.12) software (Fig. 3).

For each sample, the Shannon Index was calculated to assess the pollen diversity throughout the Kenslow Member (Shannon and Weaver, 1949). *Juglans*, *Nyssa* and *Symplocos* pollen-types were quantified to show the proportion of Cool-Tolerant extinct European taxa of East Asian affinity (CTEA) (Martinetto et al., 2017; Vieira et al., 2018). The relative abundance of CTEA-assigned taxa was summed at each depth. The Co-existence Approach was used to reconstruct the Mean Annual Temperature (MAT), Mean Annual Precipitation (MAP), Coldest Month Mean Temperature (CMMT) and Warmest Month Mean Temperature (WMMT) (Utescher et al., 2014). The co-existence approach is a nearest living relative technique, where each fossil taxon is assigned its nearest living relative, and the modern climate tolerances of the nearest living relatives are used to reconstruct the fossil climate (Mosbrugger and Utescher, 1997; Utescher et al., 2014). Forest-type categories (i.e.: mixed forest, riparian forests and bush swamps) were categorised based on plant community groupings in Worobiec et al. (2021); Fig. 3).

The co-existence approach was employed, given the simplicity of the technique and its ability to reconstruct seasonality (Fig. 5; Supplementary Table 2) (Utescher et al., 2014). We considered the disadvantages of the Co-existence Approach, including palaeoclimate reconstructions allow taxa with minimal relative abundance to have an equal weighting on the palaeoclimate outcome as taxa with significant relative abundances (Mosbrugger and Utescher, 1997). Furthermore, the technique reconstructs a range, rather than a mean value with upper and lower bounds, limiting reconstruction resolution (Utescher et al., 2014; Mosbrugger et al., 1994). Relict taxa i.e. *Cathaya*, *Cercidiphyllum* and *Sciadopitys* were removed as their present-day biogeography is limited, and their Neogene niches covered a larger range of palaeoenvironments (Mosbrugger et al., 1994; Figueiral et al., 1999).

4. Results

4.1. Grain size analysis and interpretation

The Kenslow Member at Bees Nest Pit comprises 112 cm of grey, silty clay, containing small and large fragments of fossil wood, with a 21 cm-thick lignite lentil at the top (Figs. 2, 4-5). Grain size analysis shows little change until 15 cm, when sand-sized particles of fossil plant remain within the lignite increase at the expense of clay. This coarsening-upwards trend does not, therefore, indicate an increase in energy of the drainage channels supplying this lacustrine environment as would be the case if there had been an influx of sand. By contrast, the presence of the lentil of lignite at the top of this clay succession probably indicates shallowing, and the development of a wetland. O'Keefe et al. (2020) similarly noted a decrease in siliclastic materials and presence of a woody band from 12.6 to 17.1 cm depth within the lignite lentil; see their Fig. 7 and Table 3.

4.2. Palynology: Zone KM19–1 (57–133 cm)

Descriptions of relative abundances in Sections 3.2 and 3.3 refer to Fig. 4-5. Informal pollen Zone KM19–1 contains an assemblage of Cupressaceae (3–16%); *Tsuga* (34–8%); *Tricolpopollenites liblarensis* (10–3%); *Quercoidites microhenrici* (1–7%); *Sciadopitys* (1–11%) and Cyrillaceae/ Clethraceae (0–4%). *Tsuga*-type achieves its highest values between 120 and 105 cm (34–27%), whilst *Betula* (10%) peaks at 125 cm. *Betula*-type then decreases from the remainder of the zone. Following peak *Tsuga* abundance, Cyrillaceae/Clethraceae (<7%), *Olea*-type (<6%), *Salix*-type (<3%) and *Tricolpopollenites ipilensis* (5%) all peak in this zone between 105 and 80 cm. Following this interval, these taxa decrease in relative abundance or become near-absent for the remainder of the zone. Between 105 and 75 cm, Cyperaceae, *Sphagnum,* and *Typha*-type all disappear from pollen zone KM19–1. In contrast, *Abies* and *Pinus*-type. Begin to increase in relative abundance between 80 and 75 cm. Pollen diversity declines from 85 cm to its lowest level for the entire record. KM19–1 shows increasing relative abundance of riparian elements become most sporadic in the woody lignite section (Fig. 4). Until 69–61 cm, *Betula*-type decreases, then begins to increase again, peaking at the end of this zone. Cupressaceae and *Sciadopitys* achieve their highest relative abundances (14% and 15%, respectively).

4.3. Palynology: Zone KM19–2 (5–57 cm)

Informal Zone KM19–2 contains an assemblage of *Pinus* (<15%); *Tricolpopollenites liblarensis* (<10%), Castaneioideae (8%), Cupressaceae (<18%) and *Betula*-type (19%). At 55 cm, *Pinus* (15%) and *Abies* (10%),

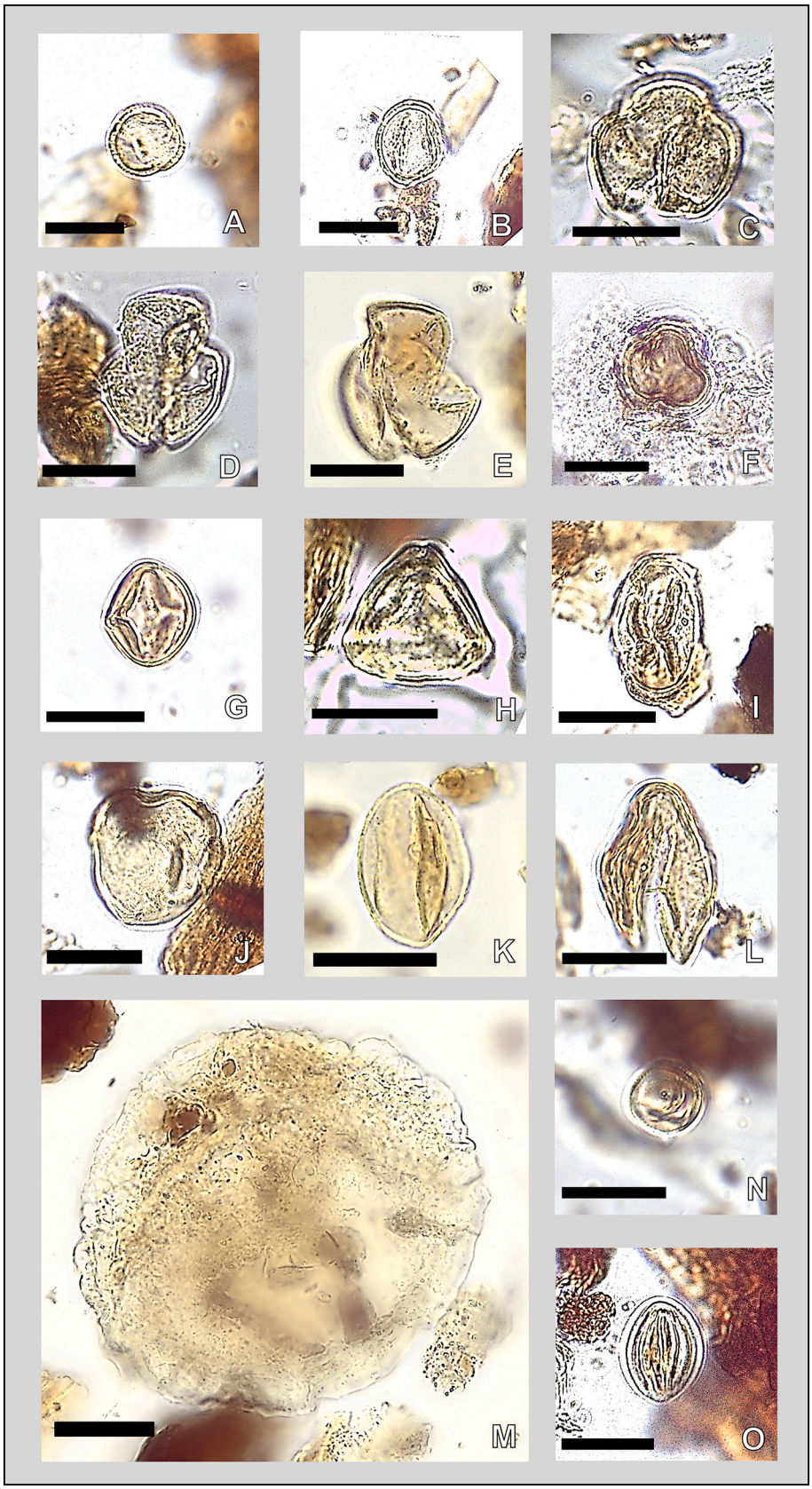

Fig. 3. Key pollen grains from the Kenslow Member at the Serravallian Best Nest Pit. All other photographs were taken from KM19–5, depth 5 cm. 3-A was taken from KM19–8, depth 8 cm. 3-G, 3-N, 3-O were taken from sample KM19–6, depth 6 cm. 3-F was taken from KM19–130, depth 130 cm. Scale bar on all scaled photographs measures 20 μm. 3-A and 3-B: *Olea*-type. 3-C: *Nyssa*-type. 3-D and 3-E: *Cercidiphyllum*-type. 3-F: Caprifoliaceae. 3-G: Cyrillaceae/ Clethraceae. 3-H: *Betula*-type. 3-I: Castaneioideae. 3-J: *Symplocos*-type. 3-K and 3-L: Cupressaceae. 3-M: *Tsuga*-type. 3-N: *Urtica*-type. 3-O: *Tricolpopollenites ipilensis.* [2-column fitting image].

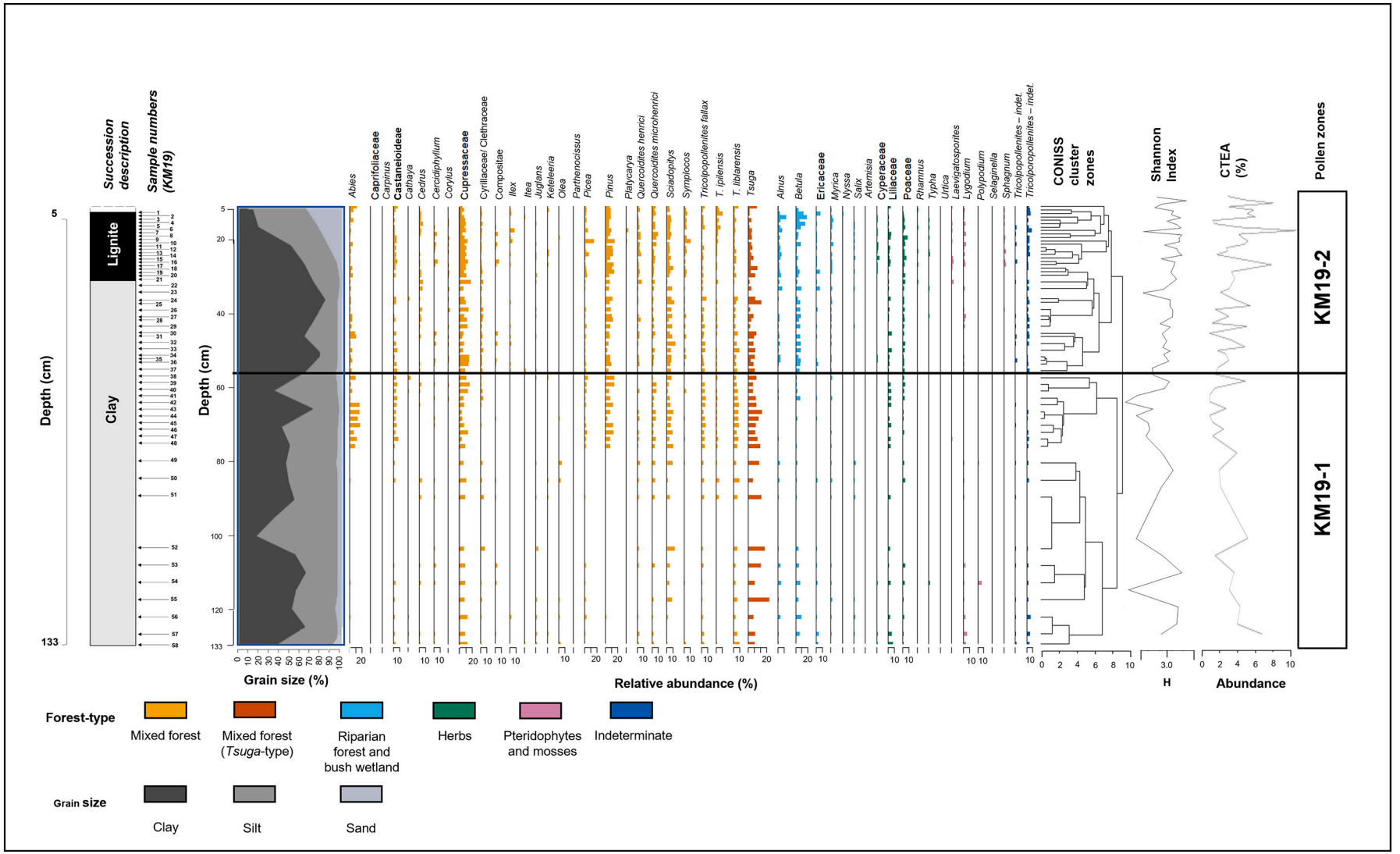

Fig. 4. Stratigraphical distribution of pollen and spores in the 58 samples of the KM19 section of the Kenslow Member from Bees Nest Pit. Pollen zones (KM19–1 and KM19–2) are defined by CONISS. The Shannon Index and CTEA (%) of each depth were calculated and plotted. Colour scheme designed to accommodate for colour-blindness. Ecological groupings are based upon Schneider (1992) and Szulc and Worobiec (2012). Sedimentology shows the grain size as measured by Mastersizer analysis. [2-column fitting image].

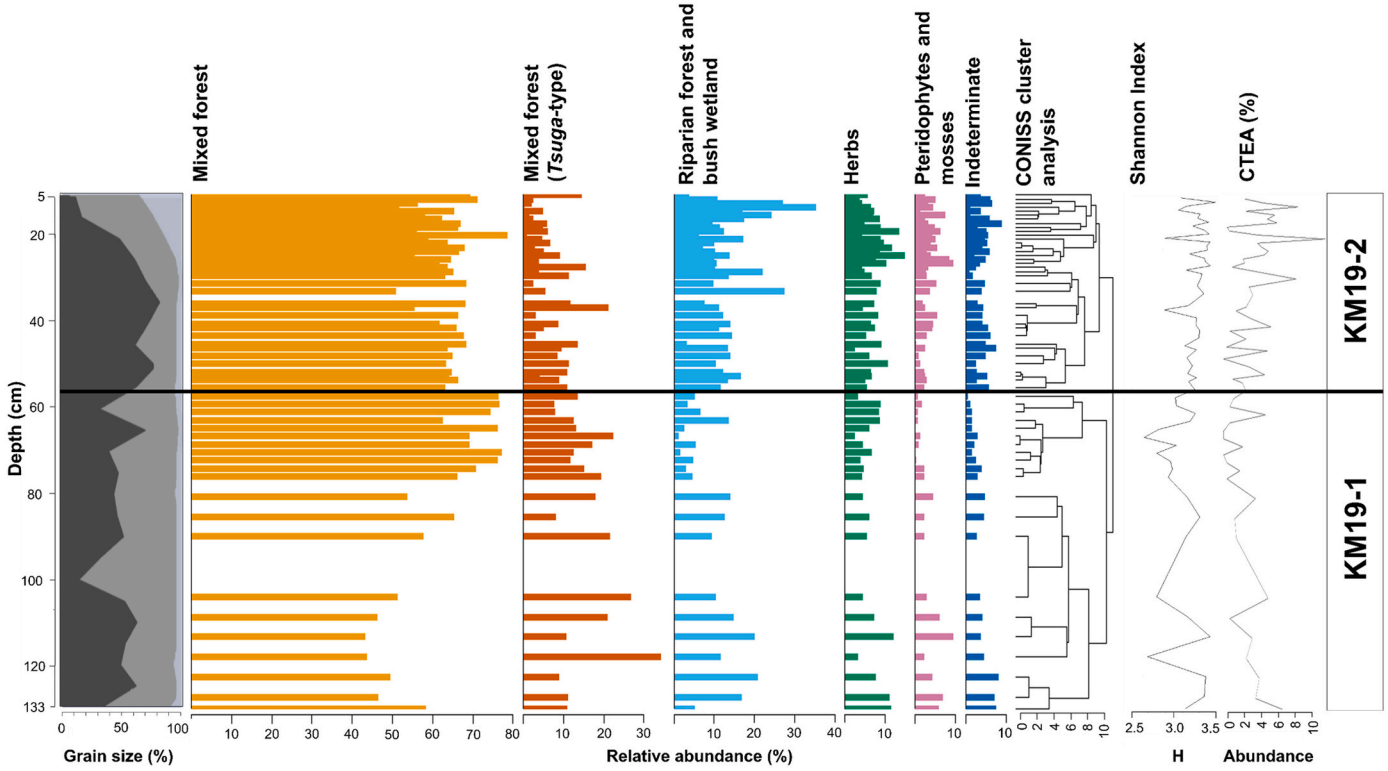

Fig. 5. Summary pollen diagram showing ecological groupings and Tsuga (dominant pollen type), with Shannon Index and relative abundance of CTEA. Colour scheme designed to accommodate for colour-blindness. Pollen zones are the same as Fig. 4. [1.5-column fitting image].

Picea (5%) and *Cathaya* (4%) relative abundances peak alongside *Tsuga* (14%). Relative abundances of Compositae and *Cercidiphyllum* peak between 42 and 45 cm at 4% and are then near-absent throughout Zone KM19–2 alongside *Abies*, which peaks between 37 and 43 cm (11%). Fig. 4 shows from 35 cm, *Sphagnum* is once again present from 38 cm, having been absent since 75 cm. Relative abundances of *Tsuga* and *Sciadopitys* peak at 33 cm (21% and 13%, respectively), with *Pinus* (12%), *Tricolpopollenites fallax* (8%), *T. liblarensis* (7%) and Castaneioideae (4%), demonstrating increasing, following relative abundances at 32 cm, alongside a reduction in the Shannon index. From 24 to 29 cm relative abundances of *Alnus* (<7%), Ericaceae (<6%) and *Cedrus* (<6%) increase. *Quercus* peaks at 27 cm (7%) alongside *Juglans*, which reaches a zonal peak from 25 to 27 cm (3%). Throughout the lignite section (5–21 cm), relative abundances of *Alnus* (<7%), *Betula* (<19%) and *Cedrus* (<4%) increase towards the surface. At 15 cm, peaks of relative abundances of *Picea* (16%) and *Pinus* (16%) occur. The increase in CTEA at 15 cm is driven by a peak in *Symplocos* (11%), and a decrease in the Shannon index value strongly suggests a low diversity zone (Fig. 4). Poaceae peaks at 14 cm (8%). *Nyssa* emerges in higher depths, peaking at 7 cm (2%). *Tricolpopollenites ipilensis,* Fabaceae-types (*T. liblarensis* and *T. fallax*) increase alongside increased numbers in the Shannon and CTEA indexes. *Tsuga* peaks in the final sample (5 cm, 15%) whereas Cupressaceae declines towards 5 cm. Relative abundance of CTEA reaches its lowest level for the entire record at 8 cm (Fig. 4). Fig. 4 shows relative abundances of Cyperaceae (<5%), *Sphagnum* (<4%) and *Typha*-types (<2%) increase towards the top of this succession. Zone KM19–2 shows increased diversity of relative abundances of taxa. KM19–2 shows increased relative abundance of angiosperms and mixed forest taxa. Relative abundance of riparian wetland elements become most sporadic in the woody lignite section (Figs. 4-5).

4.4. Palaeoclimate reconstruction

Reconstructed palaeoclimate ranges refer to those presented on Fig. 6 and in Supplementary Table 2; delimiting taxa are listed below. The co-existence approach reconstructed relatively consistent and unchanging MAT, MAP, CMMT and WMMT values. The co-existence approach reconstructs a MAT of 15.7–18.4 °C (widest reconstruction being 15.6–21.7 °C). Presence of *Picea*-types influenced the widest reconstructions of MAT (21.7 °C). Modal MAT reconstructions were delimited by *Keteleeria* and *Cedrus*. *Keteleeria* delimited modal MAP (1096 mm) reconstructions, respectively. The reconstructed CMMT was 5.0–12.5 °C (widest reconstruction being 1.8–12.5 °C), and the reconstructed WMMT was 24.7–27.9 °C (widest reconstruction being 23.6–28.3 °C). Uppermost widest WMMT reconstructions were controlled by *Quercus* relative abundance. Relative abundances of *Compositae*-types delimited the widest reconstructions of MAT (15.7 °C) and the lowermost modal CMMT and WMMT reconstructions (5 °C and 24.7 °C, respectively). Uppermost modal WMMT reconstructions considered *Nyssa* relative abundance (27.9 °C). Presence of *Symplocos*-types delimited the lower bound of the widest CMMT (1.8 °C) and WMMT (23.6 °C) reconstructions. *Cedrus*-types influenced upper modal MAT reconstructions (18.4 °C) and the lowest widest WMMT reconstructions (12.5 °C). The reconstructed MAP range was 1096–1372 mm (widest reconstruction being 703–1682 mm). MAP reconstructions were delimited by *Lygodium* (703 mm), *Olea* (1372 mm) and *Corylus* (1682 mm).

5. Discussion

The palynology of the Kenslow Member at Bees Nest Pit overall indicates a mixed mesophytic forest and a small evolving wetland environment within a wider forested landscape (Fig. 7). Reconstructed temperatures point to a warm-temperature to subtropical climate with relatively high MAP that are comparable to previously published reconstructions (Figs. 6, 8; Pound and Riding, 2016; Gibson et al., 2022).

Compared to other Serravallian co-existence approach-based MAT reconstruction from Europe, those bordering the North Atlantic are

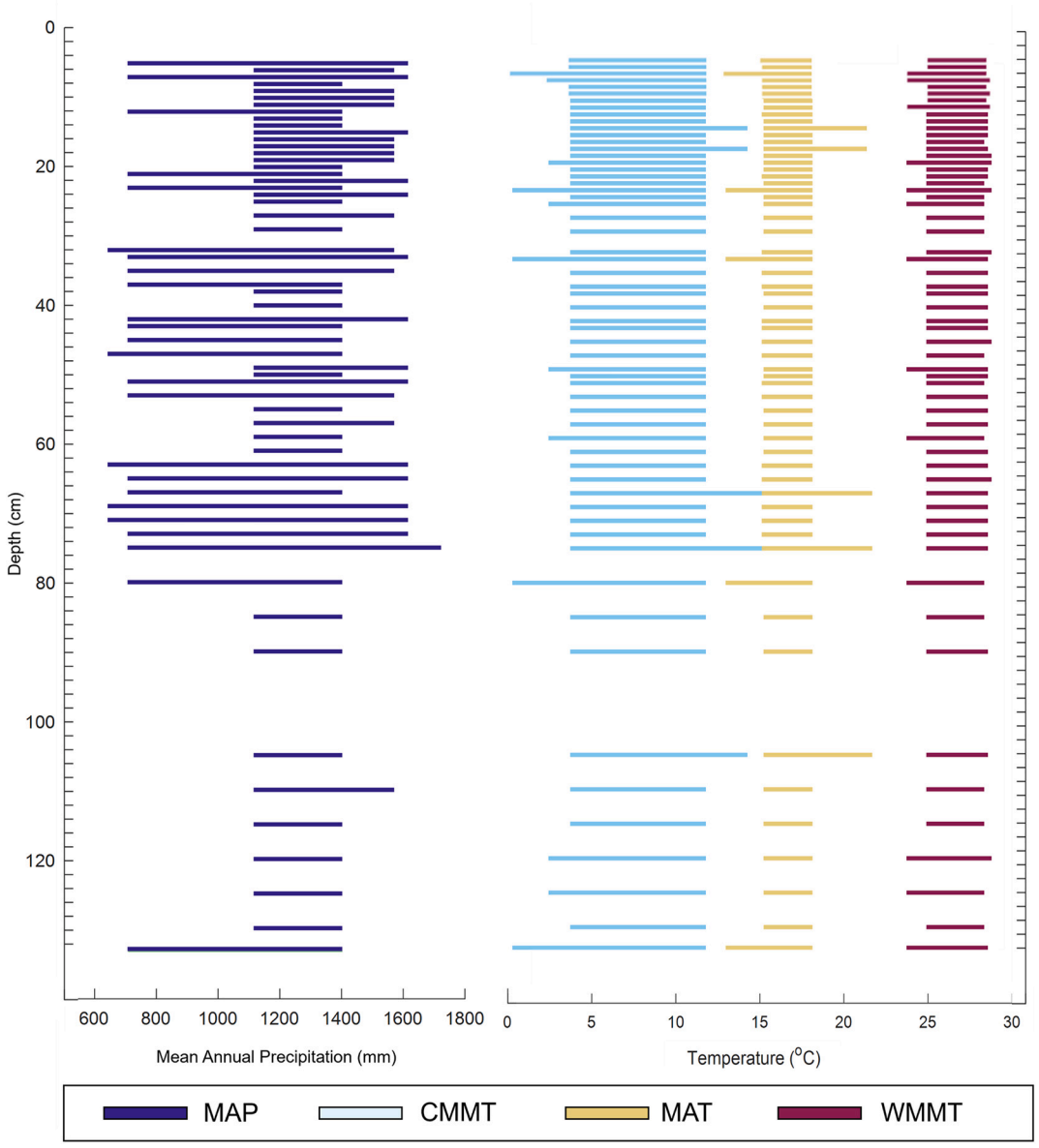

Fig. 6. Temperature and precipitation estimates through the KM19 section of the Kenslow Member, reconstructed using the co-existence approach. [1.5-column fitting image].

warmer (Fig. 8). This likely shows the influence of a proto-North Atlantic Current (Super et al., 2020). There is no evidence for substantial climate change in the section based upon the overlapping ranges of all reconstructed palaeoclimate ranges (Fig. 6). This provides additional evidence to support an environmental, rather than climatic, control on the changing pollen and spore assemblages throughout the KM19 section. However, the relatively wide ranges reconstructed for MAP and CMMT do not preclude modest changes having occurred within these variables (Fig. 6); frost-free winters occurred, like?Langhian European reconstructions (Pound and McCoy, 2021). Despite the consistent nature of the climate reconstructions, there are a number of changes in the pollen and spore sequence from the KM19 section (Figs. 4-5), in particular, there is a general transition towards autochthonous pollen-types throughout the lignite unit. Within the assemblage are elements of a *Pinus*-bog transitioning to an umbrella pine wetland with mixed mesophytic forest elements (Schneider, 1992; Fig. 7). Bush and reed-marsh mire facies elements (e.g.: *Tricolpopollenites liblarensis* and *T. fallax*) are present, indicative of a more open canopy mire environment, suggesting the Fabaceae-types had a parachthonous input of pollen (Schneider, 1992; Fig. 4; 7). The assemblages show similarities with other Miocene palaeoenvironment reconstructions in Central Europe, except for *Tsuga*-types which are typically present in only minor quantities in these assemblages – not dominant, as in KM19, suggesting a possible parauthochthonous pollen input (Schneider, 1995; Figueiral et al., 1999; Ivanov et al., 2007a; Larsson et al., 2011; Kern et al., 2012). Similar present-day assemblages exist west of the Cumberland Mountains and the Appalachian Mountains, Kentucky, North America in the Daniel Boone forest (Parker, 1985), which are dominated primarily by *Nyssa*, *Quercus* and Fagaceae, which reflect a warm-temperate mixed forests (Braun, 1942; Box, 2015). High relative abundances of coniferales (*Sciadopitys*, Cupressaceae, *Tsuga*-types) are common in Holocene-age and present-day assemblages from East Asia (Uemura, 1986; Igarashi et al., 2018).

Tsuga pollen dominates the assemblage, reaching 34% relative abundance at 120 cm (Figs. 4-5; Fig. 7: Stages A-B). Extant species of *Tsuga* require high humidity and are not tolerant of drought or fire (Thompson et al., 1999; Fusco, 2010). High relative abundances of *Tsuga* pollen are not common in European Miocene assemblages (Figueiral

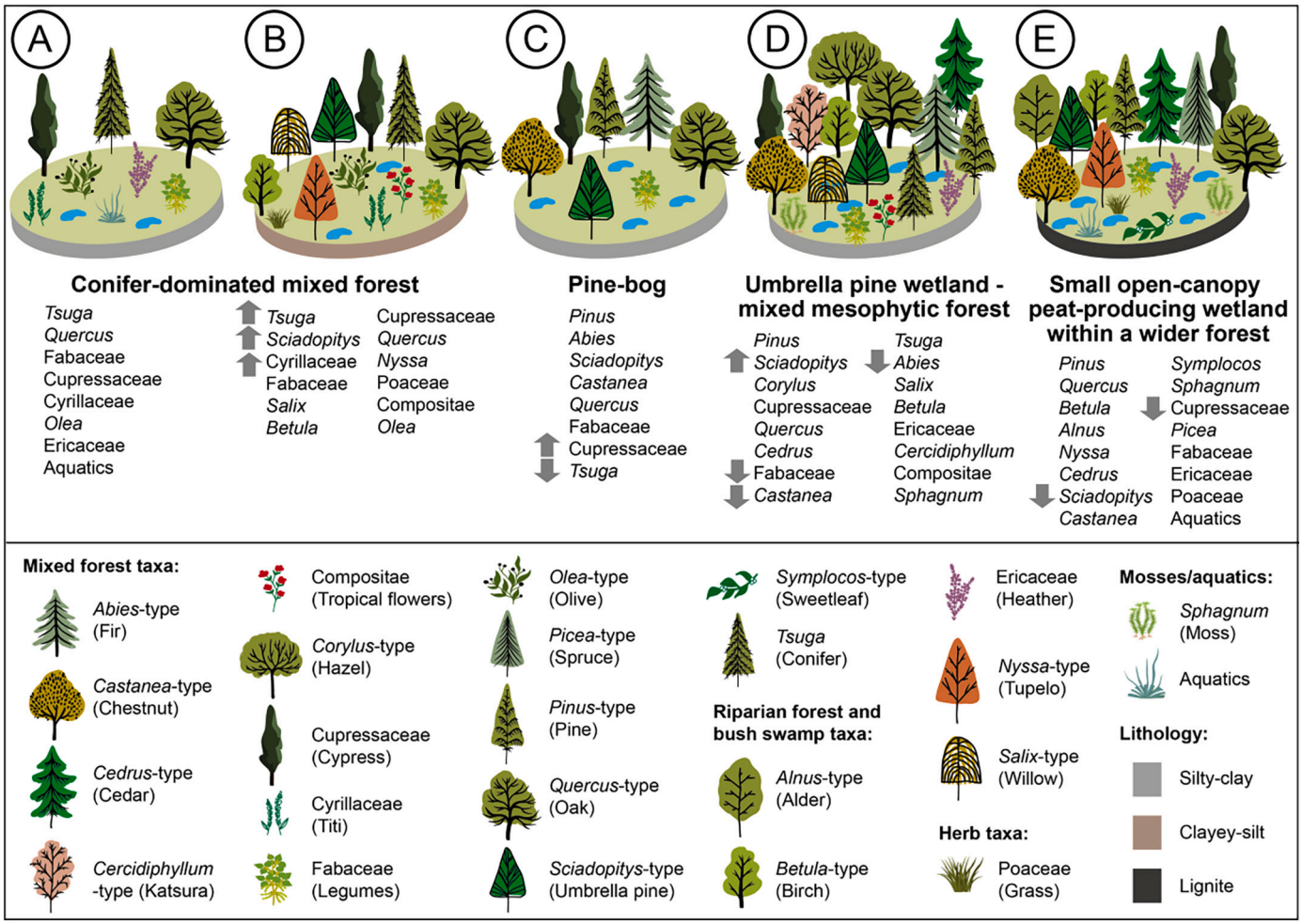

Fig. 7. The main vegetation and sediment grain size changes observed throughout pollen zones KM19–1 (A-C) and KM19–2 (C-E), shown in Figs. 4-5. The transition zone between pollen zones is apparent in C; E represents the lignite exclusively. From base to top: stages A-C represent a conifer-dominated mixed forest; stage C reconstructs a pine-dominated bog, stage D represents an umbrella pine wetland and with mixed mesophytic forest elements, and stage E shows the reconstruction of a small open-canopy peat-producing wetland within a wider forest palaeoenvironment. Increases and decreases in relative abundances are indicated by grey arrows. Key taxa are grouped into four main groups, including: mixed forest taxa; riparian forest and bush wetland taxa; herb taxa, and mosses and aquatics. [2-column fitting image].

et al., 1999; Pound et al., 2012b; Pound and Riding, 2016). Maximum amounts of 10% were previously reported for the Kenslow Member (Pound and Riding, 2016). High relative abundance of *Tsuga*-types with *Sciadopitys*-types occurs in coniferous forest assemblages of the uppermost Miocene–Pliocene Poznań Clays of Poland (Piwocki and Ziembińska-Tworzydło, 1997; Fig. 4). Although *Pinus* pollen is not present until nearly the end of pollen zone KM19–1, high relative abundance of *Pinus* pollen in the Poznań Clays is coeval with high *Tsuga* and *Sciadopitys* counts (Piwocki and Ziembińska-Tworzydło, 1997, Fig. 4). In the Poznań Clays, this is coeval with high *Pinus*-type pollen, while at Bees Nest, *Pinus*-type pollen is not present until nearly the end of the pollen zone KM19–1, when a pine-dominant bog type was present (Fig. 7).

Following peak abundance of *Tsuga* pollen, at 105 cm, there is an interval of peat-producing wetlanddevelopment (Fig. 7: Stage B). This assemblage is characterised by wet-tolerant *Salix, Sciadopitys*, *Nyssa* and *Myrica*-types which together are suggestive of wetland margin or perhaps domed conditions, allowing for the allochthonous deposition of pollen, transported via a water system (Dai et al., 2020). Conditions are like those in ombrotrophic peatlands formed in Amazonian floodplains and East Asian peatlands, which are sustained by high precipitation rates and mycorrhizal fungal-floral relationships (Lähteenoja et al., 2009; Page et al., 2010; Dai et al., 2020). The occurrence of the shrub *Itea*-type (from 53 cm) is also suggestive of a small understory within the wetland environments, proximal to the depositional basin, as the shrub's modern preferred habitats range from wetlands to stream and lake margins (Fig. 4; Ivanov et al., 2007a).

Cyrillaceae/ Clethraceae, Ericaceae, *Myrica* and *Ilex* relative abundances are highest and most consistent in KM19–1, compared to their respective relative abundances in KM19–2 (Figs. 4-5) and are resemblant of assemblages found within modern mires found from Virginia to northern Florida, USA (Richardson, 2003; Worobiec et al., 2021). Assuming comparability with North American present-day assemblages, *Myrica*-types will have affinity to *Morella caroliniensis* (Wilbur, 1994, 2002). Pollen Zone KM19–1 is entirely in the clay layer with large fragments of wood, and alternates between silty-clay and clayey-silt grain sizes (Fig. 4; Fig. 7: Stages A-C). In sedimentological terms, this could be indicative of a floodplain setting, given the implied decrease in fluvial transport capacity associated with plant fragments and lignite, as described by Joniak et al. (2020). The pollen assemblages show that the hinterland of the lake was covered by a conifer-dominated mixed forest (Schneider, 1992; Fig. 7: Stages A-B). Although not yet fully studied, the fossil wood shows extensive evidence for fungal decay and subaerial cracking (O'Keefe et al., 2020). Previous fungal remains, extracted from a sediment-filled crack in one fossil wood specimen, contain saprobic taxa that required submerged environments (Pound et al., 2019). This provides some additional evidence for an environment where previously

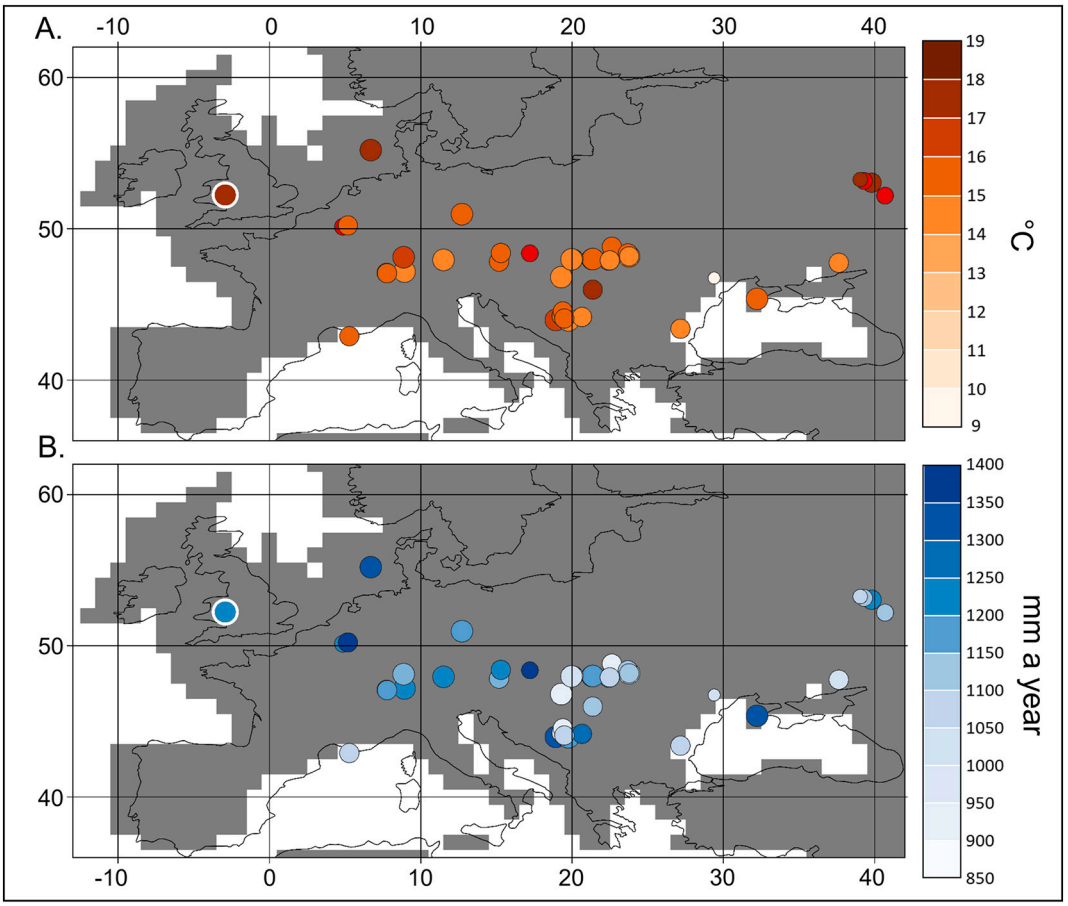

Fig. 8. Palaeogeographical maps of co-existence approach-derived palaeoclimate values across Europe for the Serravallian (Middle Miocene). A = Mean Annual Temperature and B = Mean Annual Precipitation. Because the co-existence approach reconstructs a range, the colour of the dot corresponds to the mid-point of the range, and the size of the dot indicates the range size (bigger dots = smaller ranges). The new Kenslow Member values are shown by the circle with a white outline. The base map palaeogeography is representative of the Middle Miocene (Scotese and Wright, 2018), and has the modern coastline superimposed for reader orientation. The modern latitude and longitude follows that of Hunter et al. (2013). List of localities highlighted by circles in the above figure is part of a dataset which is currently in review, as part of another paper. See section Data Availability for study site coordinates and MAP and MAT ranges of each locality. [1.5-column fitting image].

exposed dead wood became incorporated into the peat. The development of a more open canopy wetland could be due to development of a gap in the conifer dominated mixed forest, often resultant of fire regimes (Gates, 1942; Schwintzer, 1981), though without reported charcoal abundance, claims are merely suggestive (Rius et al., 2011; Wolf et al., 2013). A slow-rising water table resulting from wet periods may also be responsible for drowning of wet-intolerant shallow-rooted flora, which lead to increased wetland productivity (Schwintzer, 1981; Preston, 1996). This could have been achieved through individual treefalls, as suggested by Wilde and Riegel (2021), or through periodic fire (Ravazzi et al., 2005; Fusco, 2010).

Mixed mesophytic forest taxa initially dominated KM19–2 at 57 cm (75%), most influenced by coniferous pollen relative abundance, that implies the establishment of a *Pinus*-bog and then, potentially, a *Sciadopitys* raised bog at 33 cm (Schneider, 1992; Figs. 4-5). Extant Castaneioideae species can grow quickly to exploit the canopy opening prior to the establishment of other trees (Frothington, 1912; Nichols, 1913; Foster and Zebryk, 1993). Cupressaceae wetland development occurs most prominently from 29 cm (30%) (Fig. 4; Fig. 7: Stage C), with corresponding high relative abundances of *Alnus* (7%) and *Betula*-types (9%) around the wetland margin (Schneider, 1992; Larsson et al., 2011; Akyurt et al., 2016; Worobiec et al., 2021; Fig. 4). *Alnus* and *Betula* peak with increased autochthonous herbaceous pollen which lined the wetland edge as is also seen in Middle Miocene assemblages from the Adamów lignite deposit (Worobiec et al., 2021).

Increased relative abundance in Cyperaceae, *Sphagnum*-type and *Typha*-type, from 50 cm, are suggestive of developing wetland environments (Doren et al., 1997; Kern et al., 2012; Fig. 4). Extant *Nyssa*-types obligate to facultive members of wetland biomes in the present-day United States if interspecific competition from shrubs and herbs is limited. Relative abundances of warm-temperate taxa such as Compositae and *Cercidiphyllum*-type establish (45–43 cm), then decline (33 cm) to near-absent (Fig. 4; Fig. 7: Stage D). Extant *Cercidiphyllum* colonises a variety of open floodplain environments, and its sporadic relative abundance throughout KM19–2 may suggest intermittent establishment on a floodplain (Crane, 2008; Wei et al., 2010; Fig. 4; Fig. 7: Stage D). Fabaceae-types likely come from plants of both the shrub layer and the undergrowth, and has a clear affinity with previous wetland phases, given its gradual decrease in relative abundance at 39–32 cm after the development towards an umbrella pine wetland with mixed mesophytic forest elements (Szulc and Worobiec, 2012, Fig. 4; Fig. 7: Stage D).

The limited extent of the lignite layer could mean that it represents a forest hollow created by a fallen tree, or partial subsidence of the underlying karst, however, given the absence of reported aquatic lacustrine palynomorphs, claims are only proposed (Schaetzl et al., 1988; Pound et al., 2012b; Wilde and Riegel, 2021). Pioneer and lake margin taxa Cyperaceae, *Sphagnum*-type and *Typha*-type relative abundance increases in KM19–2 due to colonisation of this small wet opening (Verb and Rubino, 2012; Wilde and Riegel, 2021). Increase in *Typha*-type relative abundance suggests a stagnant environment, resulting in

increased organic matter deposition (Kvaçek, 2004; Hofmann and Zetter, 2005; Szulc and Worobiec, 2012). Biomass accumulated, leading to the deposition of a modest lignite lentil, defined by O'Keefe et al. (2013), in the upper Kenslow Member, which is reconstructed as a small open-canopy peat-producing wetland (Figs. 4-5; Fig. 7: Stages D-E). *Tsuga*-type, *Sciadopitys*-type, *Pinus*-type, *Tricolpopollenites fallax, T. liblarensis*, Castaneioideae relative abundance increases with decreased Shannon Index values, suggesting stabilised bog development between *Pinus*-bog and *Sciadopitys* raised-bog biomes from 16 cm (Schneider, 1992, Fig. 4).

By providing a new palaeobotanical record for the Middle Miocene-age sediment of the Kenslow Member, we demonstrate that Middle Miocene UK assemblages were wetter than previously anticipated despite reconstructions of open grasslands and arid conditions from Middle Miocene assemblages from the Madrid Basin (Prista et al., 2015; Casas-Gallego et al., 2021). Our high-precipitation palaeoclimate reconstructions were likely resultant of the developing North Atlantic Current (Jiménez-Moreno et al., 2008; Super et al., 2020). Limited seasonality, given mild CMMT reconstructions of <12.5 °C show similarities to other poorly seasonal reconstructions of Burdigalian-Langhian reconstructions across Eurasia, suggesting a possible lag in seasonality increase for higher Eurasian latitudes after the Middle Miocene Climatic Optimum (Bruch et al., 2011; Utescher et al., 2015, 2017). This period of low seasonality at mid-high Eurasian latitudes has been attributed to the likely and temporary existence of a Palaeo-Gulf Stream throughout the Middle Miocene, which also was a likely contributor to near subtropical winter?Langhian palaeoenvironments for the northwest edge of Europe (Pound and McCoy, 2021). The northwest edge of Europe shows limited step-wise cooling that is otherwise demonstrated by palaeoclimate reconstructions across inland Europe (Denk et al., 2013). Whilst it is possible that the influence of a Palaeo-Gulf Stream would dissipate circa 15 Ma, after the closure of the Central American Seaway, we attribute maintained warming to the development of the North Atlantic Current and latent and sensible heat fluxes associated with canopy cover in Miocene forest biomes (Micheels et al., 2007, 2011; Bacon et al., 2013; Montes et al., 2015; Utescher et al., 2015, 2017).

Comparison with other Miocene palaeoenvironmental reconstructions suggests an overall very inconsistent temperature gradient across central Europe, whereas high precipitation on the northwest edge of Europe remains more spatially consistent (Fig. 8). Post-Aquitanian longitudinal temperature gradients from East and West European palaeoclimate reconstructions increased throughout the Neogene, with pronounced cooling concentrated to the East, although lowest MAT reconstructions are present within Central Europe, although the main driver of this variation is influenced by the movement of the Eurasian plate, and thus biomes in northwest Europe are unaffected (Bruch et al., 2011; Popova et al., 2012; Utescher et al., 2015; Fig. 8). We highlight that the formation of the North Atlantic Current on the Atlantic peninsula likely contributed towards the stability of regional precipitation patterns on the northwest edge of Europe (Denk et al., 2013; Super et al., 2020). The influence of the North Atlantic Current on precipitation likely continued throughout the Serravallian towards the Tortonian given high precipitation reconstructions which exceeded coeval Eastern European reconstructions (Bruch et al., 2007, 2011).

We highlight that possible latitudinal shift in climate, expected resultant of 21st century climate change, may cause possible increases in temperature and precipitation – although this is not certain, given the complexity of climate mechanisms. Should increases in temperature and precipitation be observed, climatological and vegetational dynamics on the northwest edge of Europe may mimic those observed in present-day North America, particularly from the south of the Mason-Dixon line east of the Applachian Mountains, alongside trends observed in modern southeast Asia (Uemura, 1986; Balcombe et al., 2005; Igarashi et al., 2018).

6. Conclusions

From the first continuous, high-resolution pollen-spore record of the type section of the Kenslow Member at Bees Nest Pit, near Brassington, Derbyshire, UK, we report the first Miocene bog succession in the UK Neogene vegetational record. A mixed mesophytic forest with a wetland that contained a small bog developed in a warm-temperate to subtropical environment with relatively high rainfall. The bog was dominated by elements of both *Pinus*-bog and *Sciadopitys*-raised bog biomes. The two pollen zones (KM19–1 and KM19–2) indicate a transition from a *Tsuga*-dominated mixed forest to a highly-diverse shrub and tree dominated forested wetland. Increased diversity through the record resulted from the opening of the canopies that may have resulted from localised treefall, karst subsidence or floodplain dynamics. High precipitation, compared to Central Europe, on the northwest edge of Europe and frost-free conditions were likely driven by input from the proto-North Atlantic Current.

Supplementary data to this article can be found online at https://doi.org/10.1016/j.palaeo.2022.111180.

Data availability

Datasets related to this article (Fig. 8) can be found at DOI: https://doi.org/10.5281/zenodo.6817464, titled "Serravallian terrestrial climate data for Europe" hosted on Zenodo (Pound, 2022).

Declaration of Competing Interest

The authors report no conflict of interest.

Data availability

Data will be made available on request.

Acknowledgements

The fieldwork was made possible with an Elspeth Matthews Fund granted by the Geological Society to Matthew Pound in 2019. Matthew Pound thanks NERC (NE/V01501X/1) and Jennifer M.K. O'Keefe thanks NSF (award #2015813) for funding ongoing research into the Middle Miocene through the Fungi in a Warmer World (FiaWW) project. We are grateful to Jayne Spencer, the owner of Bees Nest Pit and Natural England for facilitating access to this disused quarry. Lesley Dunlop, Peter Jones, Michael Lim and Cameron Reaveley are thanked for their help with the fieldwork. Dave Thomas of Northumbria University is thanked for his assistance with the Mastersizer. James B. Riding publishes with the approval of the Director, British Geological Survey (NERC). The authors thank Torsten Utescher, Howard Falcon-Lang and an anonymous reviewer for their comments which provided very helpful insight for manuscript development.

References

Akyurt, E., Grímsson, F., Zetter, R., Leng, Q., Bouchal, J.M., 2016. Reinvestigation of the Miocene palynoflora from the Daotaiqiao Formation of north-eastern China using SEM. In: EGU Gen. Ass. Conf. Abstr.: EPSC2016-5601.

Bacon, C.D., Mora, A., Wagner, W.L., Jaramillo, C.A., 2013. Testing geological models of evolution of the Isthmus of Panama in a phylogenetic framework. Bot. J. Linn. Soc. 171 (1), 287–300. https://doi.org/10.1111/j.1095-8339.2012.01281.x.

Balcombe, C.K., Anderson, J.T., Fortney, R.H., Rentch, J.S., Grafton, W.N., Kordek, W.S., 2005. A comparison of plant communities in mitigation and reference wetlands in the mid-Appalachians. Wetlands 25 (1), 130–142. https://doi.org/10.1672/0277-5212(2005)025[0130:ACOPCI]2.0.CO;2.

Beerling, D.J., Fox, A., Anderson, C.W., 2009. Quantitative uncertainty analyses of ancient atmospheric CO2 estimates from fossil leaves. Am. J. Sci. 309 (9), 775–787. https://doi.org/10.2475/09.2009.01.

Billups, K., Schrag, D.P., 2002. Paleotemperatures and ice volume of the past 27 Myr revisited with paired Mg/Ca and 18O/16O measurements on benthic foraminifera. Paleoceanogr. 17 (1), 3-1–3-11. https://doi.org/10.1029/2000PA000567.

Boulter, M.C., 1970. Cryptomeria – a significant component of the European Tertiary. Palaeobot. B 279–287.
Boulter, M.C., 1971a. A palynological study of two of the Neogene plant beds in Derbyshire. Bull. Br. Mus. (Nat. Hist.), London 19 (7), 1–409.
Boulter, M.C., 1971b. A survey of the Neogene flora from two Derbyshire pocket deposits. Mercian Geol. 4 (1), 45–61.
Boulter, M.C., 1974. An enigmatic fossil moss from the British Tertiary. J. Bryol. 8 (1), 65–68. https://doi.org/10.1179/jbr.1974.8.1.65.
Boulter, M.C., Chaloner, W.G., 1970. Neogene fossil plants from Derbyshire (England). Rev. Palaeobot. Palynol. 10 (1), 61–78. https://doi.org/10.1016/0034-6667(70)90022-9.
Boulter, M.C., Ford, T.D., Ijtaba, M., Walsh, P.T., 1971. Brassington Formation: a newly recognized Tertiary Formation in the southern Pennines. Nat. Phys. Sci. 231 (23), 134–136. https://doi.org/10.1016/0034-6667(70)90022-9.
Box, E.O., 2015. Warm-temperate deciduous forests of Eastern North America. In: Box, E., Fujiwara, K. (Eds.), Warm-Temperate Deciduous Forests around the Northern Hemisphere. Springer, Cham, pp. 225–255. https://doi.org/10.1007/978-3-319-01261-2_13.
Braun, E.L., 1942. Forests of the Cumberland Mountains. Ecol. Monogr. 12 (4), 413–447. https://doi.org/10.2307/1943039.
Bruch, A.A., Uhl, D., Mosbrugger, V., 2007. Miocene climate in Europe—patterns and evolution: a first synthesis of NECLIME. Palaeogeogr. Palaeoclimatol. Palaeoecol. 253 (1–2), 1–7. https://doi.org/10.1016/j.palaeo.2007.03.030.
Bruch, A.A., Utescher, T., Mosbrugger, V., 2011. Precipitation patterns in the Miocene of Central Europe and the development of continentality. Palaeogeogr. Palaeoclimatol. Palaeoecol. 304 (3–4), 202–211. https://doi.org/10.1016/j.palaeo.2010.10.002.
Casas-Gallego, M., Postigo-Mijarra, J.M., Rivas-Carballo, M.R., Valle-Hernández, M.F., Morín-de Pablos, J., Barrón, E., 2021. Early evidence of continental aridity and open-habitat grasslands in Europe as revealed by the Middle Miocene microflora of the Madrid Basin. Palaeogeogr. Palaeoclimatol. Palaeoecol. 581, 110603 https://doi.org/10.1016/j.palaeo.2021.110603.
Crane, D., 2008. Effects of Land Cover on Aquatic Communities and Food Webs: A Study of Second Order Streams in Southeastern Michigan (Doctoral dissertation), pp. 1–45.
Dai, S., Bechtel, A., Eble, C.F., Flores, R.M., French, D., Graham, I.T., Hood, M.M., Hower, J.C., Korasidis, V.A., Moore, T.A., Püttmann, W., Wei, Q., Zhao, L., O'Keefe, J.M.K., 2020. Recognition of peat depositional environments in coal: a review. Int. J. Coal Geol. 219, 103383 https://doi.org/10.1016/j.coal.2019.103383.
Denk, T., Grimm, G.W., Grímsson, F., Zetter, R., 2013. Evidence from" Köppen signatures" of fossil plant assemblages for effective heat transport of Gulf Stream to subarctic North Atlantic during Miocene cooling. Biogeosci. 10 (12), 7927–7942. https://doi.org/10.5194/bg-10-7927-2013.
Doren, R.F., Armentano, T.V., Whiteaker, L.D., Jones, R.D., 1997. Marsh vegetation patterns and soil phosphorus gradients in the Everglades ecosystem. Aquat. Bot. 56 (2), 145–163. https://doi.org/10.1016/S0304-3770(96)01079-0.
Figueiral, I., Mosbrugger, V., Rowe, N.P., Ashraf, A.R., Utescher, T., Jones, T.P., 1999. The Miocene peat-forming vegetation of northwestern Germany: an analysis of wood remains and comparison with previous palynological interpretations. Rev. Palaeobot. Palynol. 104 (3–4), 239–266. https://doi.org/10.1016/S0034-6667(98)00059-1.
Flower, B.P., Kennett, J.P., 1994. The middle Miocene climatic transition: East Antarctic ice sheet development, deep ocean circulation and global carbon cycling. Palaeogeogr. Palaeoclimatol. Palaeoecol. 108 (3–4), 537–555. https://doi.org/10.1016/0031-0182(94)90251-8.
Ford, T.D., Jones, J.A., 2007. The geological setting of the mineral deposits at Brassington and Carsington, Derbyshire. Peak District Mines Historical Society 16 (5), 1–23.
Foster, D.R., Zebryk, T.M., 1993. Long-term vegetation dynamics and disturbance history of a Tsuga-dominated forest in New England. Ecol. 74 (4), 982–998. https://doi.org/10.2307/1940468.
Frothington, E.H., 1912. Second-growth hardwoods in Connecticut. In: Issue 96 of Bulletin (United States. Forest Service), 96 pp.
Fusco, F., 2010. Picea+ Tsuga pollen record as a mirror of oxygen isotope signal? An insight into the Italian long pollen series from Pliocene to early Pleistocene. Quat. Int. 225 (1), 58–74. https://doi.org/10.1016/j.quaint.2009.11.038.
Gates, F.C., 1942. The bogs of northern lower Michigan. Ecol. Monogr. 12, 213–254. https://doi.org/10.2307/1943542.
Gibson, M.E., McCoy, J., O'Keefe, J.M., Nuñez Otaño, N.B., Warny, S., Pound, M.J., 2022. Reconstructing Terrestrial Paleoclimates: a Comparison of the Co-Existence Approach, Bayesian and Probability Reconstruction Techniques using the UK Neogene. Paleoceanogr. Paleoclimatol. 37 (2) https://doi.org/10.1029/2021PA004358 e2021PA004358.
Harzhauser, M., Piller, W.E., 2007. Benchmark data of a changing sea—palaeogeography, palaeobiogeography and events in the Central Paratethys during the Miocene. Palaeogeogr. Palaeoclimatol. Palaeoecol. 253 (1–2), 8–31. https://doi.org/10.1016/j.palaeo.2007.03.031.
Hofmann, C.C., Zetter, R., 2005. Reconstruction of different wetland plant habitats of the Pannonian Basin System (Neogene, Eastern Austria). Palaios 20 (3), 266–279. https://doi.org/10.2110/palo.2002.p02-22.
Holbourn, A., Kuhnt, W., Schulz, M., Flores, J.A., Andersen, N., 2007. Orbitally-paced climate evolution during the middle Miocene "Monterey" carbon-isotope excursion. Earth Planet. Sci. Lett. 261 (3–4), 534–550. https://doi.org/10.1016/j.epsl.2007.07.026.
Hui, Z., Li, J., Xu, Q., Song, C., Zhang, J., Wu, F., Zhao, Z., 2011. Miocene vegetation and climatic changes reconstructed from a sporopollen record of the Tianshui Basin, NE Tibetan Plateau. Palaeogeogr. Palaeoclimatol. Palaeoecol. 308 (3–4), 373–382. https://doi.org/10.1016/j.palaeo.2011.05.043.
Hunter, S.J., Haywood, A.M., Valdes, P.J., Francis, J.E., Pound, M.J., 2013. Modelling equable climates of the late cretaceous: can new boundary conditions resolve data–model discrepancies? Palaeogeogr. Palaeoclimatol. Palaeoecol. 392 https://doi.org/10.1016/j.palaeo.2013.08.009, 41-51 pp.
Igarashi, Y., Irino, T., Sawada, K., Song, L., Furota, S., 2018. Fluctuations in the East Asian monsoon recorded by pollen assemblages in sediments from the Japan Sea off the southwestern coast of Hokkaido, Japan, from 4.3 Ma to the present. Glob. and planet. 163, 1–9.
IPCC, 2022. In: Pörtner, H.-O., Roberts, D.C., Tignor, M., Poloczanska, E.S., Mintenbeck, K., Alegría, A., Craig, M., Langsdorf, S., Löschke, S., Möller, V., Okem, A., Rama, B. (Eds.), Climate Change 2022: Impacts, Adaptation, and Vulnerability. Contribution of Working Group II to the Sixth Assessment Report of the Intergovernmental Panel on Climate Change. Cambridge University Press (In Press).
Ivanov, D., Ashraf, A.R., Utescher, T., Mosbrugger, V., Slavomirova, E., 2007a. Late Miocene vegetation and climate of the Balkan region: palynology of the Beli Breg Coal Basin sediments. Geol. Carpath. 58 (4), 367–381.
Ivanov, D., Bozukov, V., Koleva-Rekalova, E., 2007b. Late Miocene flora from SE Bulgaria: vegetation, landscape and climate reconstruction. Phytol. Balc. 13 (3), 281–292.
Jiménez-Moreno, G., Fauquette, S., Suc, J.P., 2008. Vegetation, climate and palaeoaltitude reconstructions of the Eastern Alps during the Miocene based on pollen records from Austria, Central Europe. J. Biogeogr. 35 (9), 1638–1649. https://doi.org/10.1111/j.1365-2699.2008.01911.x.
Joniak, P., Šujan, M., Fordinál, K., Braucher, R., Rybár, S., Kováčová, M., Kováč, M., Aumaître, G., Bourlès, D.L., Keddadouche, K., 2020. The age and paleoenvironment of a late Miocene floodplain alongside Lake Pannon: Rodent and mollusk biostratigraphy coupled with authigenic 10Be/9Be dating in the northern Danube Basin of Slovakia. Palaeogeogr. Palaeoclimatol. Palaeoecol. 538, 109482 https://doi.org/10.1016/j.palaeo.2019.109482.
Kern, A.K., Harzhauser, M., Soliman, A., Piller, W.E., Gross, M., 2012. Precipitation driven decadal scale decline and recovery of wetlands of Lake Pannon during the Tortonian. Palaeogeogr. Palaeoclimatol. Palaeoecol. 317, 1–12. https://doi.org/10.1016/j.palaeo.2011.11.021.
Kürschner, W.M., Kvacek, Z., Dilcher, D.L., 2008. The impact of Miocene atmospheric carbon dioxide fluctuations on climate and the evolution of terrestrial ecosystems. Proc. Natl. Acad. Sci. 105 (20), 449–453. https://doi.org/10.1073/pnas.0708588105.
Kvaçek, Z., 2004. Early Miocene freshwater and swamp ecosystems of the Most Basin (northern Bohemia) with particular reference to the Bílina Mine section. J. Geosci. 49 (1–2), 1–40.
Lähteenoja, O., Ruokolainen, K., Schulman, L., Alvarez, J., 2009. Amazonian floodplains harbour minerotrophic and ombrotrophic peatlands. CATENA 79 (2), 140–145. https://doi.org/10.1016/j.catena.2009.06.006.
Larsson, L.M., Dybkjær, K., Rasmussen, E.S., Piasecki, S., Utescher, T., Vajda, V., 2011. Miocene climate evolution of northern Europe: a palynological investigation from Denmark. Palaeogeogr. Palaeoclimatol. Palaeoecol. 309 (3–4), 161–175. https://doi.org/10.1016/j.palaeo.2011.05.003.
Martinetto, E., Momohara, A., Bizzarri, R., Baldanza, A., Delfino, M., Esu, D., Sardella, R., 2017. Late persistence and deterministic extinction of "humid thermophilous plant taxa of East Asian affinity" (HUTEA) in southern Europe. Palaeogeogr. Palaeoclimatol. Palaeoecol. 467, 211–231. https://doi.org/10.1016/j.palaeo.2015.08.015.
Micheels, A., Bruch, A.A., Uhl, D., Utescher, T., Mosbrugger, V., 2007. A late Miocene climate model simulation with ECHAM4/ML and its quantitative validation with terrestrial proxy data. Palaeogeogr. Palaeoclimatol. Palaeoecol. 253 (1–2), 251–270. https://doi.org/10.1016/j.palaeo.2007.03.042.
Micheels, A., Bruch, A.A., Eronen, J., Fortelius, M., Harzhauser, M., Utescher, T., Mosbrugger, V., 2011. Analysis of heat transport mechanisms from a late Miocene model experiment with a fully-coupled atmosphere–ocean general circulation model. Palaeogeogr. Palaeoclimatol. Palaeoecol. 304 (3–4), 337–350. https://doi.org/10.1016/j.palaeo.2010.09.021.
Montes, C., Cardona, A., Jaramillo, C., Pardo, A., Silva, J.C., Valencia, V., Ayala, C., Pérez-Angel, L.C., Rodriguez-Parra, L.A., Ramirez, V., Niño, H., 2015. Middle Miocene closure of the central American seaway. Sci. 348 (6231), 226–229. https://doi.org/10.1126/science.aaa2815.
Mosbrugger, V., Utescher, T., 1997. The coexistence approach—a method for quantitative reconstructions of Tertiary terrestrial palaeoclimate data using plant fossils. Palaeogeogr. Palaeoclimatol. Palaeoecol. 134 (1–4), 61–86. https://doi.org/10.1016/S0031-0182(96)00154-X.
Mosbrugger, V., Gee, C.T., Belz, G., Ashraf, A.R., 1994. Three-dimensional reconstruction of an in-situ Miocene peat forest from the lower Rhine Embayment, northwestern Germany—new methods in palaeovegetation analysis. Palaeogeogr. Palaeoclimatol. Palaeoecol. 110 (3–4), 295–317. https://doi.org/10.1016/0031-0182(94)90089-2.
Nichols, G.E., 1913. The vegetation of Connecticut II, Virgin forests. Torreya 13 (9), 199–215.
O'Keefe, J.M.K., Bechtel, A., Christanis, K., Dai, S., DiMichele, W.A., Eble, C.F., Esterle, J.S., Mastalerz, M., Raymond, A.L., Valentim, B.V., Wagner, N.J., 2013. On the fundamental difference between coal rank and coal type. Int. J. Coal Geol. 118, 58–87. https://doi.org/10.1016/j.coal.2013.08.007.
O'Keefe, J.M.K., Pound, M.J., Riding, J.B., Vane, C.H., 2020. Cellular preservation and maceral development in lignite and wood from the Brassington Formation (Miocene), Derbyshire, UK. Int. J. Coal Geol. 222, 103452 https://doi.org/10.1016/j.coal.2020.103452.
Page, S., Wust, R., Banks, C., 2010. Past and present carbon accumulation and loss in Southeast Asian peatlands. PAGES News 18 (1), 25–26.

Parker, A.J., 1985. Compositional gradients in mesophytic forests of eastern North America. Phys. Geogr. 6 (3), 247–259. https://doi.org/10.1080/02723646.1985.10642274.
Piwocki, M., Ziembińska-Tworzydło, M., 1997. Neogene of the Polish Lowlands-lithostratigraphy and pollen-spore zones. Geol. Q. 41 (1), 21–40.
Popova, S., Utescher, T., Gromyko, D., Bruch, A., Mosbrugger, V., 2012. Palaeoclimate evolution in Siberia and the Russian Far East from the Oligocene to Pliocene–evidence from fruit and seed floras. Turk. J. Earth Sci. 21 (2), 315–334. https://doi.org/10.3906/yer-1005-6.
Pound, M.J., 2022. Serravallian terrestrial climate data for Europe. Zenodo. https://doi.org/10.5281/zenodo.6817464.
Pound, M.J., McCoy, J., 2021. Palaeoclimate reconstruction and age assessment of the Miocene flora from the Trwyn y Parc solution pipe complex of Anglesey, Wales, UK. Palynol. 45 (4), 697–703. https://doi.org/10.1080/01916122.2021.1916636.
Pound, M.J., Riding, J.B., 2016. Palaeoenvironment, palaeoclimate and age of the Brassington Formation (Miocene) of Derbyshire, UK. J. Geol. Soc. 173 (2), 306–319. https://doi.org/10.1144/jgs2015-050.
Pound, M.J., Haywood, A.M., Salzmann, U., Riding, J.B., Lunt, D.J., Hunter, S.J., 2011. A Tortonian (late Miocene, 11.61–7.25 Ma) global vegetation reconstruction. Palaeogeogr. Palaeoclimatol. Palaeoecol. 300 (1–4), 29–45. https://doi.org/10.1016/j.palaeo.2010.11.029.
Pound, M.J., Haywood, A.M., Salzmann, U., Riding, J.B., 2012a. Global vegetation dynamics and latitudinal temperature gradients during the Mid to late Miocene (15.97–5.33 Ma). Earth-Sci. Rev. 112 (1–2), 1–22. https://doi.org/10.1016/j.earscirev.2012.02.005.
Pound, M.J., Riding, J.B., Donders, T.H., Daskova, J., 2012b. The palynostratigraphy of the Brassington Formation (Upper Miocene) of the southern Pennines, Central England. Palynol. 36 (1), 26–37. https://doi.org/10.1080/01916122.2011.643066.
Pound, M.J., O'Keefe, J.M., Otaño, N.B.N., Riding, J.B., 2019. Three new Miocene fungal palynomorphs from the Brassington Formation, Derbyshire, UK. Palynol. 43 (4), 596–607.
Pound, M.J., O'Keefe, J.M., Marret, F., 2021. An overview of techniques applied to the extraction of non-pollen palynomorphs, their known taphonomic issues and recommendations to maximize recovery. Geol. Soc. Lond., Spec. Publ. 511 (1), 63–76.
Preston, D.P., 1996. Harvesting Effects on the Hydrology of Wet Pine Flats (Doctoral Dissertation, Virginia Tech). Blacksburg, Virginia, pp. 1–126.
Prista, G.A., Agostinho, R.J., Cachão, M.A., 2015. Observing the past to better understand thefuture: a synthesis of the Neogene climate in Europe and its perspectives on present climate change. Open Geosci. 7 (1), 65–83. https://doi.org/10.1515/geo-2015-0007.
Quaijtaal, W., Donders, T.H., Persico, D., Louwye, S., 2014. Characterising the middle Miocene Mi-events in the Eastern North Atlantic realm: a first high-resolution marine palynological record from the Porcupine Basin. Palaeogeogr. Palaeoclimatol. Palaeoecol. 399, 140–159. https://doi.org/10.1016/j.palaeo.2014.02.017.
Ravazzi, C., Pini, R., Breda, M., Martinetto, E., Muttoni, G., Chiesa, S., Confortini, F., Egli, R., 2005. The lacustrine deposits of Fornaci di Ranica (late Early Pleistocene, Italian Pre-Alps): stratigraphy, palaeoenvironment and geological evolution. Quat. Int. 131 (1), 35–58. https://doi.org/10.1016/j.quaint.2004.07.021.
Richardson, C.J., 2003. Pocosins: hydrologically isolated or integrated wetlands on the landscape? Wetl. 23 (3), 563–576.
Riding, J.B., 2021. A guide to preparation protocols in palynology. Palynol. 45 (sup1), 1–110. https://doi.org/10.1080/01916122.2021.1878305.
Riding, J.B., Kyffin-Hughes, J.E., 2006. Further testing of a non-acid palynological preparation procedure. Palynol. 30 (1), 69–87. https://doi.org/10.1080/01916122.2006.9989619.
Rius, D., Vannière, B., Galop, D., Richard, H., 2011. Holocene fire regime changes from multiple-site sedimentary charcoal analyses in the Lourdes basin (Pyrenees, France). Quat. Sci. Rev. 30 (13–14), 1696–1709. https://doi.org/10.1016/j.quascirev.2011.03.014.
Royer, D.L., 2001. Stomatal density and stomatal index as indicators of paleoatmospheric CO2 concentration. Rev. Palaeobot. Palynol. 114 (1–2), 1–28. https://doi.org/10.1016/S0034-6667(00)00074-9.
Schaetzl, R.J., Burns, S.F., Johnson, D.L., Small, T.W., 1988. Tree uprooting: review of impacts on forest ecology. Veg. 79 (3), 165–176. https://doi.org/10.1007/BF00044908.
Schneider, W., 1992. Floral successions in Miocene swamps and bogs of Central Europe. Z. Geol. Wiss. 20, 555–570.
Schneider, W., 1995. Palaeohistological studies on Miocene brown coals of Central Europe. Int. J. Coal. Geol. 28 (2–4), 229–248. https://doi.org/10.1016/0166-5162(95)00019-4.
Schwintzer, C.R., 1981. Vegetation and nutrient status of northern Michigan bogs and conifer swamps with a comparison to fens. Can. J. Bot. 59 (5), 842–853. https://doi.org/10.1139/b81-118.
Scotese, C.R., Wright, N., 2018. PALEOMAP paleodigital elevation models (PaleoDEMS) for the Phanerozoic. Paleomap Proj 1–26.
Shannon, C.E., Weaver, W., 1949. The Mathematical Theory of Communication. The University of Illinois Press, Urbana, p. 117.
Smith, A., 2013. Digital Geological Map of Great Britain, information notes, 2013, British Geological Survey Open Report, OR/13/007: 54 pp.
Steinthorsdottir, M., Vajda, V., Pole, M., 2019. Significant transient pCO2 perturbation at the New Zealand Oligocene-Miocene transition recorded by fossil plant stomata. Palaeogeogr. Palaeoclimatol. Palaeoecol. 515, 152–161. https://doi.org/10.1016/j.palaeo.2018.01.039.
Steinthorsdottir, M., Jardine, P.E., Rember, W.C., 2020. Near-Future pCO_2 during the hot Miocene Climatic Optimum. Paleoceanogr. Paleoclimatol. 36 https://doi.org/10.1029/2020PA003900 e2020PA003900.
Steinthorsdottir, M., Coxall, H.K., De Boer, A.M., Huber, M., Barbolini, N., Bradshaw, C. D., Burls, N.J., Feakins, S.J., Gasson, E., Henderiks, J., Holbourn, A.E., 2021. The Miocene: the future of the past. Paleoceanogr. Paleoclimatol. 36 (4) https://doi.org/10.1029/2020PA004037 e2020PA004037.
Stuchlik, L., Ziembińska-Tworzydło, M., Kohlman-Adamska, A., Grabowksa, I., Ważyńska, H., Słodkowska, B., Sadowska, A., 2001. In: Stuchlik, L. (Ed.), Volume 1 – Spores In Atlas of pollen and spores of the Polish Neogene. W. Szafer Institute of Botany, Polish Academy of Sciences, Kraków, pp. 1–158. ISBN: 83-85444-79-3.
Stuchlik, L., Ziembińska-Tworzydło, M., Kohlman-Adamska, A., Grabowksa, I., Ważyńska, H., Sadowska, A., 2002. In: Stuchlik, L. (Ed.), Volume 2- Gymnosperms In Atlas of pollen and spores of the Polish Neogene. W. Szafer Institute of Botany, Polish Academy of Sciences, Kraków, pp. 1–237. ISBN: 83-85444-92-0.
Stuchlik, L., Ziembińska-Tworzydło, M., Kohlman-Adamska, A., Grabowksa, I., Słodkowska, B., Ważyńska, H., Sadowska, A., 2009. In: Stuchlik, L. (Ed.), Volume 3 – Angiosperms (1) In Atlas of pollen and spores of the Polish Neogene. W. Szafer Institute of Botany, Polish Academy of Sciences, Kraków, pp. 1–235. ISBN: 978- 83-89648-74-7.
Stuchlik, L., Ziembińska-Tworzydło, M., Kohlman-Adamska, A., Grabowksa, I., Słodkowska, B., Worobiec, E., Durska, E., 2014. In: Stuchlik, L. (Ed.), Volume 4 – Angiosperms (2) In Atlas of pollen and spores of the Polish Neogene. W. Szafer Institute of Botany, Polish Academy of Sciences, Kraków, pp. 1–466. ISBN: 978-83-62975- 23-5.
Super, J.R., Thomas, E., Pagani, M., Huber, M., O'Brien, C., Hull, P.M., 2018. North Atlantic temperature and pCO2 coupling in the early-middle Miocene. Geol. 46 (6), 519–522. https://doi.org/10.1130/G40228.1.
Super, J.R., Thomas, E., Pagani, M., Huber, M., O'Brien, C.L., Hull, P.M., 2020. Miocene evolution of North Atlantic Sea surface temperature. Paleoceanogr. Paleoclimatol. 35 (5) https://doi.org/10.1029/2019PA003748 e2019PA003748.
Szulc, J., Worobiec, E., 2012. Neogene karst sinkhole and its deposits from Górażdże Quarry, Upper Silesia-archive for palaeoenvironmental reconstructions. Ann. Soc. Geol. Pol. 82 (4), 371–385.
Thompson, R.S., Anderson, K.H., Bartlein, P.J., 1999. Atlas of relations between climatic parameters and distributions of important trees and shrubs in NorthAmerica. In: USGS Professional Paper, 650A&B.
Uemura, K., 1986. A note on Tertiary Sciadopitys (Coniferopsida) from Japan. Bull. Natn. Sci. Mus, Tokyo, Series C 12, 53–60.
Utescher, T., Bruch, A.A., Erdei, B., François, L., Ivanov, D., Jacques, F.M.B., Kern, A.K., Mosbrugger, V., Spicer, R.A., 2014. The Coexistence Approach—theoretical background and practical considerations of using plant fossils for climate quantification. Palaeogeogr. Palaeoclimatol. Palaeoecol. 410, 58–73. https://doi.org/10.1016/j.palaeo.2014.05.031.
Utescher, T., Bondarenko, O.V., Mosbrugger, V., 2015. The Cenozoic Cooling–continental signals from the Atlantic and Pacific side of Eurasia. Earth Planet. Sci. Lett. 415, 121–133. https://doi.org/10.1016/j.epsl.2015.01.019.
Utescher, T., Dreist, A., Henrot, A.J., Hickler, T., Liu, Y.S.C., Mosbrugger, V., Portmann, F.T., Salzmann, U., 2017. Continental climate gradients in North America and Western Eurasia before and after the closure of the central American Seaway. Earth Planet. Sci. Lett. 472, 120–130. https://doi.org/10.1016/j.epsl.2017.05.019.
Utescher, T., Ashraf, A.R., Kern, A.K., Mosbrugger, V., 2021. Diversity patterns in microfloras recovered from Miocene brown coals of the lower Rhine Basin reveal distinct coupling of the structure of the peat-forming vegetation and continental climate variability. Geol. J. 56 (2), 768–785. https://doi.org/10.1002/gj.3801.
Van Dam, J.A., 2006. Geographic and temporal patterns in the late Neogene (12–3 Ma) aridification of Europe: the use of small mammals as paleoprecipitation proxies. Palaeogeogr. Palaeoclimatol. Palaeoecol. 238 (1–4), 190–218. https://doi.org/10.1016/j.palaeo.2006.03.025.
Velitzelos, D., Bouchal, J.M., Denk, T., 2014. Review of the Cenozoic floras and vegetation of Greece. Rev. Palaeobot. Palynol. 204, 56–117. https://doi.org/10.1016/j.revpalbo.2014.02.006.
Verb, R.G., Rubino, D.L., 2012. A preliminary survey of diatom taxa from old-growth forest tip-up pools in Southeastern Indiana flatwoods. Proc. Indiana Acad. Sci. 121 (1), 1–7.
Vieira, M., Pound, M.J., Pereira, D.I., 2018. The late Pliocene palaeoenvironments and palaeoclimates of the western Iberian Atlantic margin from the Rio Maior flora. Palaeogeogr. Palaeoclimatol. Palaeoecol. 495, 245–258. https://doi.org/10.1016/j.palaeo.2018.01.018.
Walsh, P.T., Boulter, M.C., Ijtaba, M., Urbani, D.M., 1972. The preservation of the Neogene Brassington Formation of the southern Pennines and its bearing on the evolution of Upland Britain. J. Geol. Soc. 128 (6), 519–559.
Walsh, P.T., Collins, P., Ijtaba, M., Newton, J.P., Scott, N.H., Turner, P.R., 1980. Palaeocurrent directions and their bearing on the origin of the Brassington Formation (Miocene-Pliocene) of the southern Pennines, Derbyshire, England. Mercian Geol. 8 (1), 47–61.
Walsh, P.T., Atkinson, K., Boulter, M.C., Shakesby, R.A., 1987. The Oligocene and miocene outliers of West Cornwall and their bearing on the geomorphological evolution of Oldland Britain. Philosophical Transactions of the Royal Society of London Ser. A, Math. Phys. Sci. 211–245.
Walsh, P.T., Banks, V.J., Jones, P.F., Pound, M.J., Riding, J.B., 2018. A reassessment of the Brassington Formation (Miocene) of Derbyshire, UK and a review of related hypogene karst suffosion processes. J. Geol. Soc. 175 (3), 443–463. https://doi.org/10.1144/jgs2017-029.
Wei, X.Z., Jiang, M.X., Huang, H.D., Yang, J.Y., Yu, J., 2010. Relationships between environment and mountain riparian plant communities associated with two rare

tertiary-relict tree species, Euptelea pleiospermum (Eupteleaceae) and Cercidiphyllum japonicum (Cercidiphyllaceae). Flor. Morphol., Distrib., Funct. Ecol Plants 205 (12), 841–852.
Wilbur, R.L., 1994. The Myricaceae of the United States and Canada: genera, subgenera, and series. SIDA, Contrib. Bot 93–107.
Wilbur, R.L., 2002. The identity and history of Myrica caroliniensis (Myricaceae). Rhodora 31–41.
Wilde, V., Riegel, W., 2021. A middle Eocene treefall pit and its filling: a microenvironmental study from the onset of a forest mire in the Geiseltal (Germany). Palaeobiodiv. Palaeoenv. 1–15. https://doi.org/10.1007/s12549-021-00501-3.
Wolf, M., Lehndorff, E., Wiesenberg, G.L., Stockhausen, M., Schwark, L., Amelung, W., 2013. Towards reconstruction of past fire regimes from geochemical analysis of charcoal. Org. Geochem. 55, 11–21. https://doi.org/10.1016/j.orggeochem.2012.11.002.
Worobiec, E., Widera, M., Worobiec, G., Kurdziel, B., 2021. Middle Miocene palynoflora from the Adamów lignite deposit, Central Poland. Palynology 45 (1), 59–71. https://doi.org/10.1080/01916122.2019.1697388.
Yorke, C., 1954. The Pocket Deposits of Derbyshire. Birkenhead, Three Volumes. Privately Published by the Author, 113 pp.
Yorke, C., 1961. The Pocket Deposits of Derbyshire: A General Survey. Privately Published by the Author, Birkenhead.